

# Rectangular amplitudes, conformal blocks, and applications to loop models

Roberto Bondesan<sup>1,2</sup>, Jesper L. Jacobsen<sup>1,3</sup> and Hubert Saleur<sup>2,4</sup>

<sup>1</sup>LPTENS, École Normale Supérieure, 24 rue Lhomond, 75231 Paris, France

<sup>2</sup> Institute de Physique Théorique, CEA Saclay, F-91191 Gif-sur-Yvette, France

<sup>3</sup>Université Pierre et Marie Curie, 4 place Jussieu, 75252 Paris, France

<sup>4</sup> Physics Department, USC, Los Angeles, CA 90089-0484, USA

## Abstract

In this paper we continue the investigation of partition functions of critical systems on a rectangle initiated in [R. Bondesan *et al*, Nucl.Phys.B862:553-575,2012]. Here we develop a general formalism of rectangle boundary states using conformal field theory, adapted to describe geometries supporting different boundary conditions. We discuss the computation of rectangular amplitudes and their modular properties, presenting explicit results for the case of free theories. In a second part of the paper we focus on applications to loop models, discussing in details lattice discretizations using both numerical and analytical calculations. These results allow to interpret geometrically conformal blocks, and as an application we derive new probability formulas for self-avoiding walks.

## 1 Introduction

The study of conformal field theories (CFT) on a rectangle, while relying on a well known theoretical framework, offers interesting technical challenges, and had not been considered much in the literature until quite recently. In the last few years, the topic has however received increased attention, both in the context of open string field theory[22, 23, 37], and in the context of condensed matter physics applications. The latter include study of quantum quenches for systems with open boundary conditions [6, 15], or the study of transport properties in disordered network models [4, 10].

For a CFT on a rectangle, the topology is trivial, while there are sharp corners, and in general four different boundary conditions on the four edges, see figure 1.

The most natural way to calculating properties—such as partition functions—in this geometry relies on a concept of “fully open” boundary state, which was introduced in

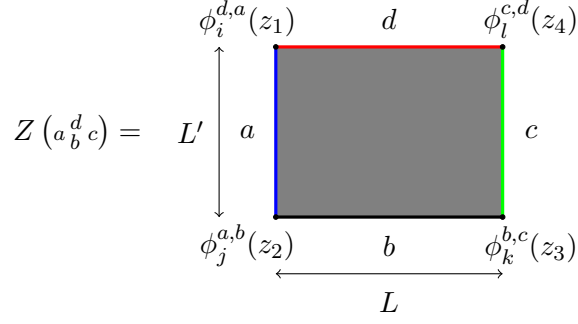


Figure 1: The partition function for a CFT on a rectangle. Different boundary conditions are imposed on each side, and boundary condition changing operators are inserted at the corners  $z_i$ .

[3]. In the special case where all boundary conditions are the same, this state was studied in details in [3], and related to remarkable algebraic properties of the Virasoro algebra. In the same reference, the correspondence between the CFT and lattice model descriptions of the rectangle geometry was also considered in details. The present paper is a continuation of this work, where we now consider the case of different boundary conditions.

The first two sections delineate the general formalism. In section 2 we introduce the most general fully open boundary states  $|B_{ac}^b\rangle$  and discuss their general expression in terms of *basis states*  $|i^s_j\rangle$ , which are the natural analog of the Ishibashi states [24] in this context. In section 3, we study amplitudes (partition functions), and compare the approaches using the open boundary states with the approach using conformal mappings and conformal blocks. Various checks and related results are considered in section 4 where we discuss free theories.

We then turn in section 5 to our main motivation for this work, which is the calculation of partition functions for loop models of statistical mechanics with lines inserted at the corners, for an example see figure 2. These objects have potential relations with transport properties of network models as well as potential probabilistic applications. They also provide a natural tool to investigate degeneracy issues when the corresponding conformal field theory becomes logarithmic [32, 33]. Although the conformal field theoretic description of loop models is not fully understood, we are able to find out the detailed connection between the general considerations of the first part of this paper and boundary conditions defined geometrically. This allows us to interpret conformal blocks in terms of loops, and calculate the desired partition functions. We find in particular

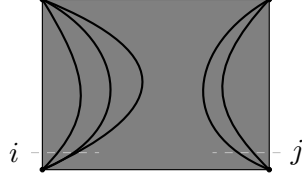


Figure 2: A schematic illustration of the partition function for a loop model where we insert  $i$  lines in the bottom left corner and  $j$  in the bottom right one, and we impose that  $s = i + j$  lines propagate vertically.

that coefficients in geometrical amplitudes for percolation, dilute or dense polymers are then related with indecomposability parameters.

A few final remarks are gathered in the conclusion, while some technical points are addressed in the appendices.

## 2 Solutions of the gluing condition for semi-rectangular geometries

A boundary condition in conformal field theory has to preserve conformal symmetry. This is encoded in the so-called gluing conditions for the stress tensor of the CFT, gluing left- and right-moving modes. In the familiar case of a theory defined on a disk, this implies that

$$(L_n - \bar{L}_{-n}) |B^p\rangle = 0, \quad (1)$$

where  $|B^p\rangle$  is the boundary state describing the boundary of the disk.  $|B^p\rangle$  is an element of the space of states  $F$  of the bulk theory which we assume to decompose onto Virasoro irreducibles  $V_i$  with multiplicities  $N_{ij}$ ,  $F = \bigoplus_{ij} N_{ij} V_i \otimes \bar{V}_j$ . The condition (1) can be solved in each direct summand separately and the unique solution in  $V_i \otimes \bar{V}_i$  is given by so-called Ishibashi states [24]:

$$|i\rangle\rangle = \sum_N |i; N\rangle \otimes \overline{|i; N\rangle}, \quad (2)$$

with  $|i; N\rangle$  ( $\overline{|i; N\rangle}$ ) an orthonormal base of  $V_i$  ( $\bar{V}_i$ ).

Using the transformation law of the stress tensor, also more complicated boundaries can be described by gluing conditions. In [3] the geometry of the bottom of the rectangle, see figure 3, was considered. In this case not only left and right movers are glued together, but also positive and negative modes within a chiral algebra. Further, conformal anomalies coming from singularities of the stress tensor at the corners will show up

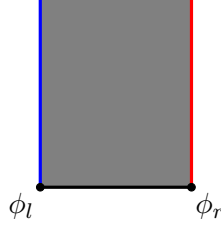


Figure 3: The semi-rectangular geometry defining the boundary state.

in the gluing condition. Consider the possibility of having different boundary conditions whose change is mediated by fields inserted in the left and right corners of the bottom of the rectangle, of weights respectively  $h_l$  and  $h_r$ . Then, denoting the boundary state  $|B^o\rangle$ , the gluing condition reads:

$$\left( L_n - L_{-n} - 2n \left( \tilde{h}_l + (-)^n \tilde{h}_r \right) \right) |B^o\rangle = 0. \quad (3)$$

where

$$\tilde{h} = 2h - \frac{c}{16}, \quad (4)$$

$c$  being the central charge.

The rectangle bottom in the  $\zeta$ -plane, with corners say in  $\zeta = -1, 0$ , can be mapped to the region  $\mathcal{D} = \{z \in \mathbb{C} : \Im(z) > 0, |z| > 1\}$ , left of figure 4, by  $z = e^{-i\pi\zeta}$ . This geometry is the appropriate one to discuss boundary states in radial quantization, and clearly the gluing condition (and thus the boundary state) is not changed with respect to that for the bottom of the rectangle. In [3] the operator implementing algebraically the mapping from the upper half plane to the geometry with corners  $\mathcal{D}$ , mapping  $z = \pm 1$  to  $w = \pm 2$ , see figure 4, was found. It has the following product formula:

$$\hat{G}_{\mathcal{D}} = \lim_{N \rightarrow \infty} e^{-\frac{1}{2^{N-1}} L_{-2^N}} \dots e^{-\frac{1}{2} L_{-4}} e^{-L_{-2}}. \quad (5)$$

It follows that when  $h_l = h_r = 0$ , homogeneous boundary conditions, the boundary state is:

$$|B^o\rangle = \hat{G}_{\mathcal{D}} |0\rangle \quad (6)$$

$$= |0\rangle - L_{-2}|0\rangle - \frac{1}{2}L_{-4}|0\rangle + \frac{1}{2}L_{-2}^2|0\rangle + \dots \quad (7)$$

We will comment about the normalization of the state  $|B^o\rangle$  when we compute the amplitudes involving boundary states below. In the following we will continue to use the normalization fixed in equation (6).

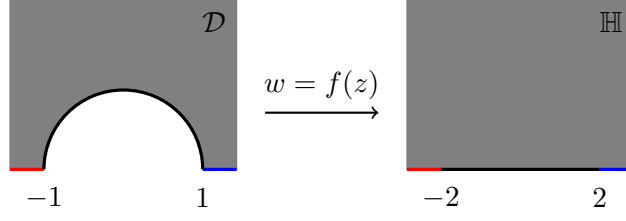


Figure 4: Mapping of semicircular region  $\mathcal{D}$  to the upper half plane  $\mathbb{H}$ .  $f$  is the Joukowski map:  $f(z) = z + z^{-1}$ .

In this paper we focus on the case of different boundary conditions on the sides of the semi-rectangle. To make things concrete, call the condition on the left side  $a$ , that on the bottom  $b$  and that on the right  $c$ . Boundary condition changing (BCC) operators  $\phi_i^{a|b}$ ,  $\phi_j^{b|c}$ —which can be identified with the lowest eigenstate of the Hamiltonian on a strip with boundary conditions  $a$  and  $b$  on the sides—will then sit at the left and right corners. We denote the boundary state we want to determine  $|B_{ac}^b\rangle$ , which is thus associated graphically to:

$$|B_{ac}^b\rangle = a \begin{array}{c} | \\ \bullet \\ b \end{array} \begin{array}{c} | \\ \bullet \\ c \end{array} \quad (8)$$

If  $X = \Phi(z_1, \bar{z}_1) \cdots \phi(x) \cdots$  is a chain of arbitrary bulk and boundary operators,  $|B_{ac}^b\rangle$  is defined by

$$\langle X \rangle_{\mathcal{D}} = \langle 0 | X | B_{ac}^b \rangle, \quad (9)$$

where  $\langle X \rangle_{\mathcal{D}}$  is the correlator in the geometry  $\mathcal{D}$ . The operator  $\hat{G}_{\mathcal{D}}$  introduced above by definition implements at the operator level the conformal map from  $\mathcal{D}$  to  $\mathbb{H}$ , so that we have:

$$\langle X \rangle_{\mathcal{D}} = \langle 0 | \tilde{X} \phi_i^{a|b}(-2) \phi_j^{b|c}(2) | 0 \rangle, \quad (10)$$

where we defined  $\tilde{X} = \hat{G}_{\mathcal{D}}^{-1} X \hat{G}_{\mathcal{D}}$  (if  $\hat{G}_{\mathcal{D}} = e^{\sum_n \epsilon_n L_n}$ , then  $\hat{G}_{\mathcal{D}}^{-1} = e^{-\sum_n \epsilon_n L_n}$ ), and the right term is a correlation function on the upper half plane. Since the out-vacuum  $\langle 0 |$  is invariant under this mapping, one has

$$|B_{ac}^b\rangle = \hat{G}_{\mathcal{D}} \phi_i^{a|b}(-2) \phi_j^{b|c}(2) | 0 \rangle. \quad (11)$$

We now recall the boundary OPE of two boundary fields (see e.g. [28],  $x > y$ ):

$$\phi_i^{a,b}(x) \phi_j^{b,c}(y) = \sum_s (x-y)^{h_s-h_i-h_j} C_{ijs}^{abc} \phi_s^{a,c}\left(\frac{x+y}{2}\right) + \dots \quad (12)$$

The boundary OPE coefficients  $C_{ijs}^{abc}$  are part of the known data of the CFT [17, 34]:

$$C_{ijs}^{abc} = F_{bs} \begin{bmatrix} a & c \\ i & j \end{bmatrix}, \quad (13)$$

where the  $F$ -matrices relate conformal blocks in different bases [31]. We will see explicit examples below. Note that from taking different OPEs of the three point function  $\langle \phi_i^{ab} \phi_j^{bc} \phi_k^{ca} \rangle$  one has the cyclic relation

$$C_{ijk}^{abc} C_{kk0}^{aca} = C_{jki}^{bca} C_{ii0}^{aba}. \quad (14)$$

Further, the normalization of the identity  $\phi_0$  (0 is the label for the identity) is fixed by demanding  $\phi_0^{aa} \phi_i^{ab} = \phi_i^{ab}$ , which implies

$$C_{0ij}^{aab} = \delta_{ij}, \quad (15)$$

for every  $a, i$ . More properties can be found in [28, 34].

Eq. (11) can then be written as:

$$|B_{ac}^b\rangle = \sum_s C_{ijs}^{abc} \sqrt{C_{ss0}^{aca}} |i \begin{smallmatrix} s \\ j \end{smallmatrix} \rangle, \quad (16)$$

where we defined the *basis states*  $|i \begin{smallmatrix} s \\ j \end{smallmatrix} \rangle$  by

$$|i \begin{smallmatrix} s \\ j \end{smallmatrix} \rangle := \hat{G}_{\mathcal{D}} 4^{h_s - h_i - h_j} \sum_{n \geq 0} \sum_{\gamma \vdash n} 4^n \beta_{i,j}^{s,\gamma} L_{-\gamma} |\phi_s\rangle \quad (17)$$

$$= 4^{h_s - h_i - h_j} \left[ |\phi_s\rangle + \sum_{n \geq 1} \sum_{\gamma \vdash n} \delta_{i,j}^{s,\gamma} L_{-\gamma} |\phi_s\rangle \right], \quad (18)$$

where  $\gamma \vdash n$  is a partition  $(\gamma_1, \dots, \gamma_L)$  of  $n$ , and we used the shorthand  $L_{-\gamma} := L_{-\gamma_1} \cdots L_{-\gamma_L}$ . The coefficients  $\beta_{i,j}^{s,\gamma}$  appear in the OPE of (bulk) chiral fields  $\phi_i, \phi_j$  in the term corresponding to the descendant of  $s$ ,  $L_{-\gamma} \phi_s$  (We use the notations of [18], section 6.6.3 of this reference, although we simplify the notation by writing  $\gamma$  instead of  $\{\gamma\}$ ). The term  $\sqrt{C_{ss0}^{aca}}$  in eq. (16) is needed in order to define the basis state as an element of the Verma module of the primary  $\phi_s$  without any information about the boundary conditions. Alternatively one could remove the factor  $\sqrt{C_{ss0}^{aca}}$  and define the basis state as an element of the Verma module of  $\phi_s^{a,c}$ , where  $\langle \phi_s^{a,c} | \phi_s^{c,a} \rangle = C_{ss0}^{aca}$ .

The basis states  $|i \begin{smallmatrix} s \\ j \end{smallmatrix} \rangle$  span the space of boundary states solving eq. (3) and are the analogues for the rectangular geometry of Ishibashi states (2). For determining the coefficients  $\delta$ 's in eq. (18) one could work out the algebra in (17) or directly solve the constraint (3) for different values of  $n$ . It is well-known however that the combinatorics of the Virasoro algebra is complicated and does not allow to get a closed formula for

the coefficients in the above expansions, be it  $\beta_{i,j}^{s,\gamma}$  or  $\delta_{i,j}^{s,\gamma}$ . An exception is the case of free theories, when the Virasoro generators admit an expression in terms of bosonic or fermionic oscillators, see the discussion in section 4. In general, there is therefore the following difference between Ishibashi states for the cylinder geometry and the basis states for the rectangle: rectangle basis states depend on the boundary operators inserted at the corners, so on their fusion, which does not give access to an explicit expression. Instead Ishibashi states are known explicitly from eq. (2).

The state  $|B_{ac}^b\rangle$  is directly given by a single basis state if the fusion  $\phi_i^{a,b} \otimes \phi_j^{b,c}$  produces only one channel. This is of course the case of homogeneous boundary conditions, when no BCC operators are present,

$$|B_{aa}^a\rangle = (C_{000}^{aaa})^{3/2} |0\ 0\rangle = |0\ 0\rangle = \hat{G}_{\mathcal{D}} |0\rangle, \quad (19)$$

where  $|\phi_0\rangle \equiv |0\rangle$ , and we used (15). This is also the case when there is only a single BCC operator. Indeed, if  $a = b$ , calling the BCC operator  $\phi_s^{a,c}$ , one has

$$|B_{ac}^a\rangle = C_{0ss}^{aac} \sqrt{C_{ss0}^{aca}} |0\ s\rangle \quad (20)$$

$$= \sqrt{C_{ss0}^{aca}} \hat{G}_{\mathcal{D}} \phi_s(2) |0\rangle = \sqrt{C_{ss0}^{aca}} \hat{G}_{\mathcal{D}} \exp(2L_{-1}) |\phi_s\rangle, \quad (21)$$

since  $L_{-1}$  generates translations and  $|\phi_s\rangle$  inserts the operator at the origin.  $C_{ss0}^{aca}$  is not fixed by (15) and could be set to one, see [34].

The discussion presented so far solves implicitly the problem of finding the boundary states for the rectangular geometry. In the next section we will compute amplitudes involving these states and give more explicit results. Before moving on, let us define the conjugate states of eq. (16)

$$\langle B_{ac}^b| = \sum_s C_{ijs}^{abc} \sqrt{C_{ss0}^{aca}} \langle i\ j|_s, \quad (22)$$

which are associated graphically to

$$\langle B_{ac}^b| = a \begin{array}{c} \bullet \\ \hline \bullet \end{array} \begin{array}{c} b \\ \hline \bullet \end{array} c. \quad (23)$$

$\langle i\ j|_s$  is the conjugate of  $|i\ j\rangle_s$ , and we introduce also the following graphical notation for the basis states:

$$|i\ j\rangle_s = \begin{array}{c} s \\ \hline \phi_i \quad \phi_j \end{array} \quad (24)$$

### 3 Amplitudes and conformal blocks

We consider a rectangle of length  $L'$  and width  $L$  in the  $z$ -plane, with boundary conditions  $a, b, c, d$ , so that BCC operators  $\phi_i^{a,d}(z_1), \phi_j^{a,b}(z_2), \phi_k^{b,c}(z_3), \phi_l^{d,c}(z_4)$  sit at the corners, see figure 1. The CFT partition function is by definition:

$$Z \left( \begin{smallmatrix} d \\ a & b & c \end{smallmatrix} \right) = a \left[ \begin{smallmatrix} d \\ \uparrow \\ b \end{smallmatrix} \right] c = Z_0(\tau) \langle \phi_i^{a,d}(z_1), \phi_j^{a,b}(z_2), \phi_k^{b,c}(z_3), \phi_l^{d,c}(z_4) \rangle, \quad (25)$$

where  $Z_0$  is the partition function for homogeneous boundary conditions and the correlator is evaluated on the rectangle. The arrow in the picture is the direction of imaginary time in a transfer matrix picture, which will be developed below, and  $\tau = iL'/L$ .

We recall first that  $Z_0$  has been computed in [26]:

$$Z_0(\tau) = a \left[ \begin{smallmatrix} a \\ \uparrow \\ a \end{smallmatrix} \right] a = L^{c/4} \eta^{-c/2}(\tau), \quad (26)$$

where  $\eta$  is the Dedekind eta function. Definitions and properties of the  $\eta$  function are collected in appendix A. In [3], we showed that the following relation between the boundary state (6) and this partition function exists:

$$\langle B^o | \hat{q}^{L_0 - c/24} | B^o \rangle = L^{-c/4} Z_0 = \eta(\tau)^{-c/2}, \quad (27)$$

$\hat{q}$  being the relevant combination of  $L'/L$  appearing in the strip transfer matrix:

$$\hat{q} = \sqrt{q} = \exp(\pi i \tau). \quad (28)$$

From relation (27) we note that the state  $|B^o\rangle$  is not normalizable:

$$\langle B^o | B^o \rangle = \lim_{q \rightarrow 1} \eta(\tau)^{-c/2} = \begin{cases} \infty & \text{if } c > 0, \\ 0 & \text{if } c < 0, \\ 1 & \text{if } c = 0. \end{cases} \quad (29)$$

A similar situation happens for the Ishibashi states in the cylinder geometry. However in the case of cylinder states, one can fix a possible multiplicative constant in the definition, which is not fixed by the gluing condition on the disk (1), by requiring the equality of the cylinder amplitude to the annulus partition function, see [8]. We do not know how to fix a possible multiplicative constant  $\alpha$  in the definition  $|B^o\rangle = \alpha \hat{G}_{\mathcal{D}} |0\rangle$ . This issue is related to the very definition of a partition function on a rectangle, containing the factor  $L^{c/4}$  (or  $L^w$  in the general case, see below) in (26), which depends on the unit of measure of length we adopt.

We now go back to the computation of (25). We choose the following fusion channel of BCC operators (here depicted on a segment):





It maps the points on the real line  $(-1/k, -1, 1, 1/k)$  to the corners of a rectangle with  $L = 2K$  and  $L' = K'$ ,  $(-K + iK', -K, K, K + iK')$ , where  $K$  is the complete elliptic integral of the first kind of modulus  $k$  and  $K'$  the complementary one, see figure 5.

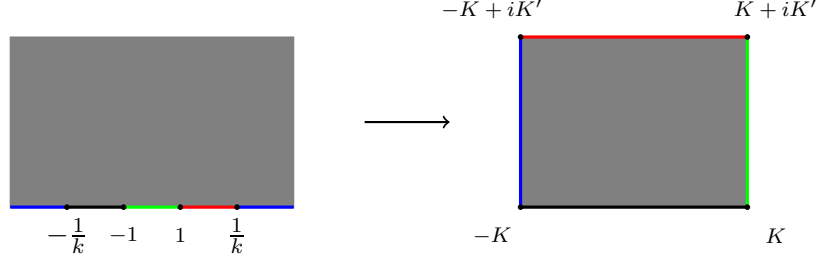


Figure 5: The Schwarz-Cristoffel transformation of eq. (37) sending the the upper half plane to the rectangle.

The Jacobian  $J$  of this transformation is singular at the corners, but when the boundary operators sit at the corners too, eq. (36) continues to hold since as the argument of the field approaches the corner in  $z_c$ , the field itself goes to zero as  $(z - z_c)^h \phi(z_c)$ , where  $h$  is the dimension of the field. Then we look at the Jacobian as the coefficient of the first term in the expansion around the position of the corners. The result is

$$J = k^{-h_i - h_l} (1 - k^2)^{h_i + h_j + h_k + h_l}. \quad (38)$$

Thanks to global conformal invariance, a chiral correlator can be written as [18]

$$\langle \phi_1(w_1) \phi_2(w_2) \phi_3(w_3) \phi_4(w_4) \rangle = \prod_{i < j} w_{ij}^{\mu_{ij}} G(\zeta), \quad \mu_{ij} = \frac{1}{3} \left( \sum_{k=1}^4 h_k \right) - h_i - h_j, \quad (39)$$

with  $\zeta$  being the anharmonic ratio ( $w_{ij} = w_i - w_j$ )

$$\zeta = \frac{w_{12} w_{34}}{w_{13} w_{24}}. \quad (40)$$

We now let  $(w_1, w_2, w_3, w_4) = (-1/k, -1, 1, 1/k)$  and we find

$$\prod_{i < j} w_{ij}^{\mu_{ij}} = \left( k^{4(h_1 + h_4) + h_2 + h_3} (2(1 - k^2))^{-(h_1 + h_2 + h_3 + h_4)} \right)^{1/3}. \quad (41)$$

Expressing everything in terms of  $\tau$ , using eq. (199), we have:

$$\langle \phi_i(z_1) \phi_j(z_2) \phi_k(z_3) \phi_l(z_4) \rangle = \left( 2^{\frac{1}{3}} \pi^2 \eta^4 (2K)^{-2} \right)^{h_i + h_j + h_k + h_l} G(\zeta). \quad (42)$$

We recognize in the above formula the term length  $L = 2K$  raised to the correct modular weight (32) coming from field insertions.  $G(\zeta)$  in general is a linear combination of

conformal blocks  $\mathcal{F}_{il;jk}^s(\zeta)$ , corresponding to the fusion channel  $s$ , and in the end eq. (33) becomes:

$$\mathcal{A}_s^{i,j,k,l}(\tau) \propto \eta(\tau)^{-2w(i,j,k,l)} \mathcal{F}_{il;jk}^s(1 - \zeta(\tau)), \quad (43)$$

where the anharmonic ratio as a function of  $\tau$  is

$$\zeta = \left( \frac{k-1}{k+1} \right)^2 = \left( \frac{\theta_4(\tau)}{\theta_3(\tau)} \right)^4. \quad (44)$$

Let us compute the constant of proportionality by demanding the normalization of the amplitude to be  $c_0 = 4^{2h_s - (h_i + h_j + h_k + h_l)}$  in eq. (34), according to eq. (18). When  $q \rightarrow 0$ ,  $1 - \zeta(\tau) \rightarrow 0$ , and using that our conventions are such that

$$\mathcal{F}_{il;jk}^s(z) \sim z^{h_s - \frac{1}{3}(h_i + h_j + h_k + h_l)}, \quad (45)$$

we have the following small- $q$  expansion of the right hand side of (43):

$$\eta(\tau)^{-2w(i,j,k,l)} \mathcal{F}_{il;jk}^s(1 - \zeta(\tau)) = 4^{2h_s - \frac{2}{3}(h_i + h_j + h_k + h_l)} q^{-c/48 + h_s/2} (1 + O(\hat{q})). \quad (46)$$

Then the exact relation is:

$$\mathcal{A}_s^{i,j,k,l}(\tau) = 4^{-\frac{1}{3}(h_i + h_j + h_k + h_l)} \eta(\tau)^{-2w(i,j,k,l)} \mathcal{F}_{il;jk}^s(1 - \zeta(\tau)). \quad (47)$$

### 3.1 Dualities and modular covariance

Duality relations act in the space of conformal blocks [31]. The F-duality states the associativity of fusion product, relating conformal blocks singular near  $\zeta = 0$  to those singular near  $\zeta = 1$ :

$$\mathcal{F}_{ij;kl}^s(\zeta) = \sum_r F_{sr} \begin{bmatrix} i & l \\ j & k \end{bmatrix} \mathcal{F}_{il;jk}^r(1 - \zeta). \quad (48)$$

Another transformation is braiding, exchanging the position of  $\phi_j$  and  $\phi_k$ :

$$\mathcal{F}_{ij;kl}^s(\zeta) = \sum_r B_{sr} \begin{bmatrix} i & l \\ j & k \end{bmatrix} \mathcal{F}_{ik;jl}^r\left(\frac{1}{\zeta}\right). \quad (49)$$

$F$ - and  $B$ -matrices satisfy several identities [31]. The relation between  $F$ -matrices and boundary OPE coefficients  $C_{ijs}^{abc}$  has been pointed out in eq. (13).

Let us remark now that the space of conformal blocks furnishes a representation of the modular group  $\Gamma = \text{PSL}(2, \mathbb{Z})$  with the following natural action:

$$M \circ \mathcal{F}(\zeta(\tau)) = \mathcal{F}(\zeta(M\tau)), \quad M \in \Gamma. \quad (50)$$

Indeed one can relate  $\zeta(M\tau)$  to  $\zeta(\tau)$  using the explicit expression of the anharmonic ratio in terms of the modular parameter, eq. (44). For the generators  $S : \tau \rightarrow -1/\tau$  and  $T : \tau \rightarrow \tau + 1$ , one has

$$\zeta(S\tau) = 1 - \zeta(\tau); \quad \zeta(T\tau) = \frac{1}{\zeta(\tau)}, \quad (51)$$

so that the action of  $T$  and  $S$  on conformal blocks is

$$S \circ \mathcal{F}_{ij;kl}^s(\zeta(\tau)) = \sum_r F_{sr} \begin{bmatrix} i & l \\ j & k \end{bmatrix} \mathcal{F}_{il;jk}^r(\zeta(\tau)) \quad (52)$$

$$T \circ \mathcal{F}_{ij;kl}^s(\zeta(\tau)) = \sum_r B_{sr} \begin{bmatrix} i & l \\ j & k \end{bmatrix} \mathcal{F}_{ik;jl}^r(\zeta(\tau)). \quad (53)$$

This action transfers immediately into modular covariance of rectangular amplitudes using eq. (47). Modular inversion  $S$  acts in an obvious way on the rectangle by interchanging its length and width. Modular translation  $T$  instead deforms it to a rhombus, and its physical meaning could be understood by using the action given in the equation above as braiding of the boundary fields. Let us see then in more details how  $\Gamma$  acts on the rectangle.  $S$ -action allows to relate amplitudes of rectangles of inverse aspect ratio as

$$S \circ \mathcal{A}_s^{i,j,k,l}(\tau) = \mathcal{A}_s^{l,i,j,k}(-1/\tau) \quad (54)$$

$$= \tau^{-w(i,j,k,l)} \sum_r F_{sr} \begin{bmatrix} i & l \\ j & k \end{bmatrix} \mathcal{A}_r^{i,j,k,l}(\tau), \quad (55)$$

where we defined

$$\mathcal{A}_s^{l,i,j,k}(-1/\tau) = \langle {}^l_s | \hat{q}^{L_0 - c/24} | {}^s_i \rangle, \quad (56)$$

with

$$\hat{q} = \sqrt{\tilde{q}} = \exp(-\pi i/\tau). \quad (57)$$

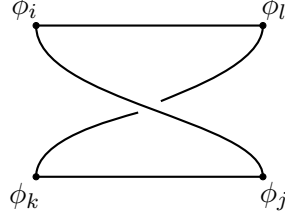
Note the appearance of the modular weight  $w(i,j,k,l)$  (not present if considering the transformation of the full CFT partition function  $Z$ , because of the relation (31)) from the transformation of  $\eta$ , see Appendix A. To see how  $T$  acts, we consider its action on the amplitude of a rectangle of inverse aspect ratio

$$T \circ \mathcal{A}_s^{i,j,k,l}(-1/\tau) = \mathcal{A}_s^{i,j,k,l}(-1/(\tau+1)) \quad (58)$$

$$= e^{i\pi w(i,j,k,l)/3} (\tau+1)^{-w(i,j,k,l)} \eta(\tau)^{-2w(i,j,k,l)} \mathcal{F}_{ij;kl}^s \left( \frac{1}{\zeta(\tau)} \right) \quad (59)$$

$$= e^{i\pi w(i,j,k,l)/3} \left( \frac{\tau+1}{\tau} \right)^{-2w(i,j,k,l)} \sum_r B_{sr} \begin{bmatrix} i & l \\ j & k \end{bmatrix} \mathcal{A}_r^{i,j,k,l}(-1/\tau). \quad (60)$$

Note that the amplitude  $\mathcal{A}_r^{i,k,j,l}(-1/\tau)$  can be thought of as the  $r$ -channel amplitude of a rectangle whose bottom, where operators  $\phi_j^{a,b}$  and  $\phi_k^{b,c}$  sit, has been twisted by  $\pi$ :



Recall that for the torus a Dehn twist by  $2\pi$  at fixed time is exactly  $T$ ; here we have  $\hat{q}$  so the twist is the half. This should be the way to understand modular translation of rectangular amplitudes. In particular if the twisted amplitude is equal to the original one, as happens when  $k = j$ , we expect to have invariance (in the sense of equation (58)) under modular translations.

More generally modular transformations are powerful tools for constraining the objects we want to compute, and their usefulness are well appreciated for the case of a CFT on cylinders and tori [7, 8]. Let us see what symmetry constraint one has on the rectangle<sup>1</sup> and how the basis state we have introduced solves it. The natural constraint comes from imposing the consistency of the partition function upon switching the direction of imaginary time from vertical to horizontal:

$$a \begin{array}{c} \bullet \\ \uparrow \\ \bullet \end{array} \begin{array}{c} d \\ \bullet \\ \bullet \end{array} c = a \begin{array}{c} \bullet \\ \rightarrow \\ \bullet \end{array} \begin{array}{c} d \\ \bullet \\ \bullet \end{array} c. \quad (61)$$

From eq. (31), the l. h. s. is

$$a \begin{array}{c} \bullet \\ \uparrow \\ \bullet \end{array} \begin{array}{c} d \\ \bullet \\ \bullet \end{array} c = L^{w(i,j,k,l)} \sum_s C_{ils}^{adc} C_{jks}^{abc} C_{ss0}^{aca} \mathcal{A}_s^{i,j,k,l}(\tau), \quad (62)$$

while the r. h. s. is

$$a \begin{array}{c} \bullet \\ \rightarrow \\ \bullet \end{array} \begin{array}{c} d \\ \bullet \\ \bullet \end{array} c = L'^{w(i,j,k,l)} \sum_s C_{ijs}^{dab} C_{kls}^{bcd} C_{ss0}^{dbd} \langle s \ l | \hat{q}^{L_0 - c/24} | i \ s \rangle \quad (63)$$

$$= L'^{w(i,j,k,l)} 4^{-\frac{1}{3}(h_i + h_j + h_k + h_l)} \sum_s C_{ijs}^{dab} C_{kls}^{bcd} C_{ss0}^{dbd} \eta(-1/\tau)^{-2w(i,j,k,l)} \quad (64)$$

$$\begin{aligned} & \times \mathcal{F}_{ij;kl}^s(1 - \zeta(-1/\tau)) \\ & = L^{w(i,j,k,l)} \sum_r \sum_s C_{ijs}^{dab} C_{kls}^{bcd} C_{ss0}^{dbd} F_{sr} \begin{bmatrix} i & l \\ j & k \end{bmatrix} \mathcal{A}_r^{i,j,k,l}(\tau). \end{aligned} \quad (65)$$

<sup>1</sup> The action of the modular group on a rectangle has been discussed in [13, 27] in the case of percolation.

Equating the coefficients of the amplitude we get the following consistency equation:

$$\sum_s C_{ijs}^{dab} C_{kls}^{bcd} C_{ss0}^{dbd} F_{sr} \begin{bmatrix} i & l \\ j & k \end{bmatrix} = C_{ilr}^{adc} C_{jkr}^{abc} C_{rr0}^{aca}. \quad (66)$$

This equation is simply stating the associativity of the fusion product of boundary fields, the so-called sewing constraint coming from crossing symmetry of correlators [28]. It has been shown in [34] that its solution is given by (13). Then, since we defined directly our boundary states in terms of physical boundary OPEs, consistency under modular inversion does not give any additional constraint. Recall that for the cylinder geometry a similar argument gives the so-called Cardy states [8].

### 3.2 Examples

We now show how to construct boundary states and associated amplitudes in some explicit examples. The case of homogeneous boundary conditions—no BCC operator insertions at the corners—has already been discussed in details in [3], and we here concentrate on the change of boundary conditions.

#### 3.2.1 Two operator insertions

The simplest case to deal with is that of two different boundary conditions around the rectangle, when two BCC operator are inserted in two corners. This computation amounts to transforming the two-point function of the BCC operators in the upper half plane to the rectangle geometry with operators in the corners and has already appeared in [26]. In this case only one channel can propagate and our formulas of section 3 are of course simplified considerably. For definiteness let us consider first the case of boundary condition  $a$  on the bottom and  $b$  on the other sides, and call  $\phi_i^{a,b}$  the BCC operator. The partition function is:

$$Z \left( \begin{smallmatrix} b & b \\ a & b \end{smallmatrix} \right) = b \begin{smallmatrix} b \\ \uparrow \\ a \end{smallmatrix} b = Z \left( \begin{smallmatrix} a & b \\ b & b \end{smallmatrix} \right) = b \begin{smallmatrix} a \\ \uparrow \\ b \end{smallmatrix} b \quad (67)$$

$$= L^{c/4-4h} \langle B_{bb}^b | \hat{q}^{L_0-c/24} | B_{bb}^a \rangle \quad (68)$$

$$= L^{c/4-4h} C_{ii0}^{aba} \mathcal{A}_0^{0,i,i,0}(\tau). \quad (69)$$

Using eq. (47), we express the amplitude using the following conformal block:

$$\mathcal{F}_{00;ii}^0(1-\zeta) = \left( \frac{\zeta}{(1-\zeta)^2} \right)^{h/3} = 4^{-4/3h} \left( \frac{\eta(\tau)}{\eta(2\tau)} \right)^{8h}, \quad (70)$$

to have:

$$Z \left( \begin{smallmatrix} b & b \\ a & b \end{smallmatrix} \right) = C_{ii0}^{aba} 4^{-2h} L^{c/4-4h} \eta(\tau)^{-c/2+16h} \eta(2\tau)^{-8h} \quad (71)$$

$$= C_{ii0}^{aba} 4^{-2h} L^{c/4-4h} q^{-c/48} \quad (72)$$

$$\times \left[ 1 + \frac{c-32h}{2} q + \left( \frac{c(6+c)}{8} - 8(2+c)h + 128h^2 \right) q^2 + \dots \right]. \quad (73)$$

Note that as expected from the symmetry of interchanging the boundary operators, this partition function is invariant (up to a phase) with respect to modular translation. Of course it is not invariant under modular inversion  $S$ , and indeed under  $S$  this partition function transforms into that for operators inserted in the left or right corners, which is:

$$Z \left( \begin{smallmatrix} b & b \\ a & b \end{smallmatrix} \right) = a \begin{smallmatrix} \bullet & b \\ \uparrow & \bullet \\ \bullet & b \end{smallmatrix} b = Z \left( \begin{smallmatrix} b & b \\ b & a \end{smallmatrix} \right) = b \begin{smallmatrix} \bullet & b \\ \uparrow & \bullet \\ \bullet & b \end{smallmatrix} a \quad (74)$$

$$= L^{c/4-4h} \langle B_{ab}^b | \hat{q}^{L_0-c/24} | B_{ab}^b \rangle \quad (75)$$

$$= L^{c/4-4h} C_{ii0}^{aba} \mathcal{A}_i^{i,i,0,0}(\tau) \quad (76)$$

$$= C_{ii0}^{aba} L^{c/4-4h} \eta(\tau)^{-c/2+16h} \eta(\tau/2)^{-8h} \quad (77)$$

$$= C_{ii0}^{aba} L^{c/4-4h} q^{-c/48+h/2} \left[ 1 + 8h\hat{q} + \frac{c+8h(8h-1)}{2} q + \dots \right]. \quad (78)$$

If instead the operators are inserted in non-adjacent corners, say in the top-left and the right-bottom one, we then have

$$Z \left( \begin{smallmatrix} b & b \\ a & a \end{smallmatrix} \right) = b \begin{smallmatrix} \bullet & b \\ \uparrow & \bullet \\ \bullet & a \end{smallmatrix} a = Z \left( \begin{smallmatrix} a & a \\ b & a \end{smallmatrix} \right) = b \begin{smallmatrix} \bullet & a \\ \uparrow & \bullet \\ \bullet & b \end{smallmatrix} a \quad (79)$$

$$= L^{c/4-4h} \langle B_{ba}^b | \hat{q}^{L_0-c/24} | B_{ba}^a \rangle \quad (80)$$

$$= L^{c/4-4h} C_{ii0}^{bab} \mathcal{A}_i^{0,i,0,i}(\tau). \quad (81)$$

The following conformal block

$$\mathcal{F}_{0i;i0}^i(1-\zeta) = (\zeta(1-\zeta))^{h/3} = 2^{4/3h} \left( \frac{\eta(2\tau)\eta(\tau/2)}{\eta(\tau)^2} \right)^{8h}, \quad (82)$$

contributes to the amplitude, and we have:

$$Z \left( \begin{smallmatrix} b & b \\ a & a \end{smallmatrix} \right) = C_{ii0}^{bab} L^{c/4-4h} \eta(\tau)^{-c/2-8h} \eta(\tau/2)^{8h} \eta(2\tau)^{8h} \quad (83)$$

$$= C_{ii0}^{bab} L^{c/4-4h} q^{-c/48+h/2} \left[ 1 - 8h\hat{q} + \frac{c+8h(8h-1)}{2} q + \dots \right]. \quad (84)$$

The above results can be also obtained by computing the overlap of the boundary states. The amplitude  $\mathcal{A}_0^{0,i,i,0}(\tau)$  involved in the partition function of eq. (67), is defined

as in eq. (33), so it will be given by the overlap of the boundary state for homogeneous boundary conditions, see eq. (19), and  $|_i^0\rangle$ , whose first levels read:

$$4^{2h}|_i^0\rangle = |0\rangle + \left(\frac{32h}{c} - 1\right)L_{-2}|0\rangle + \frac{c(22+5c) - 64(6+5c)h + 5120h^2}{2c(22+5c)}L_{-2}^2|0\rangle - \frac{c(22+5c) - 256(2+c)h + 3072h^2}{2c(22+5c)}L_{-4}|0\rangle + \dots \quad (85)$$

We have checked that  $\langle B_{bb}^b|\hat{q}^{L_0-c/24}|B_{bb}^a\rangle$  computed using the above expression of boundary states reproduces the small- $q$  expansion of eq. (73) up to order  $\hat{q}^{10}$ . The boundary states building the amplitudes of eq. (74) and (79) are given by a single basis state as in (20). Eq. (74) is given by the overlap of:

$$|_i^i\rangle = |\phi_i\rangle - 2L_{-1}|\phi_i\rangle - L_{-2}|\phi_i\rangle + 2L_{-1}^2|\phi_i\rangle + 2L_{-2}L_{-1}|\phi_i\rangle - \frac{4}{3}L_{-1}^3|\phi_i\rangle - \frac{1}{2}L_{-4}|\phi_i\rangle + \frac{1}{2}L_{-2}^2|\phi_i\rangle - 2L_{-2}L_{-1}^2|\phi_i\rangle + \frac{2}{3}L_{-1}^3|\phi_i\rangle + \dots \quad (86)$$

with itself. Instead the partition function in eq. (79) is given by  $\langle^0_i^i|\hat{q}^{L_0-c/24}|_i^i\rangle$ .  $\langle^0_i^i|$  is computed from  $\langle^i_0|$  by sending  $2 \rightarrow -2$  in the explicit formula (20) and this gives the minus signs present in equation (84) with respect to (78). Again we have verified the agreement of the series expansions using the explicit form of the boundary states up to level  $\hat{q}^{10}$ . Note that the small- $q$  expansion (73) contains only even powers of  $\hat{q}$ , as expected from left-right symmetry of the boundary conditions. Indeed odd powers are related to descendants at odd levels changing sign under inversion of the coordinates  $z \rightarrow -z$ , and thus are not allowed to propagate.

Furthermore one can check the agreement of these results with computations for free theories presented in section 4, eqs. (105), (106) and (107).

### 3.2.2 Four operator insertions

We now turn to the case of four insertions of BCC operators, and we consider the simple situation when the operators inserted are all degenerate at level 2, so that the dimension of each operator equals  $h_{1,2}$  or  $h_{2,1}$ . We make this choice since an explicit and simple expression for the conformal blocks of these fields is available [18] (actually it suffices that just one of the four fields is degenerate at level 2 to find a closed form of the conformal blocks, but we treat the case of all fields degenerate at level 2 for easiness of notation). For fixing ideas we can think of the  $Q$ -states Potts model with fixed boundary conditions on left and right boundaries and free on the top and bottom sides. Clearly we have to distinguish two situations: either the fixed spins are in an equal state  $\alpha$  or they are



different, say in states  $\alpha$  and  $\alpha'$ . These partition functions have been already discussed in details in [11] and here we reproduce the results and comment about boundary states and modular properties. Introducing the label  $i$  of the Virasoro modules  $V_{(1,1+i)}$  (or  $V_{(1+i,1)}$ ) in Kac notation, one associates to free boundary conditions on the strip the label 1, to fixed equal 0, and to fixed different 0 and 2. This is consistent with the known fusion rules [11] since  $1 \otimes 1 = 0 \oplus 2$ . Then concretely we would like to compute the partition functions

$$Z \left( \begin{smallmatrix} 1 \\ 0 & 1 & a \end{smallmatrix} \right) = 0 \begin{smallmatrix} \bullet & \frac{1}{1} & \bullet \\ \uparrow & & \uparrow \\ \bullet & & \bullet \end{smallmatrix} a, \quad a = 0, 2. \quad (87)$$

If  $a = 0$ , at the corners on the bottom there are BCC operators  $\phi_1^{0,1}$  and  $\phi_1^{1,0}$  whose OPE coefficients are clearly  $C_{1,1,s}^{0,1,0} \propto \delta_{s,0}$  so that only the identity channel propagates. For  $a = 2$  we insert instead  $\phi_1^{0,1}$  and  $\phi_1^{1,2}$  whose OPE coefficients are  $C_{1,1,s}^{0,1,2} \propto \delta_{s,2}$  so that only the  $\phi_2$ -channel is left. Calling  $h \equiv h_1$  and  $\mathcal{A}_a \equiv \mathcal{A}_a^{1,1,1}$ , we then have

$$Z \left( \begin{smallmatrix} 1 \\ 0 & 1 & a \end{smallmatrix} \right) = \tilde{\mathcal{N}}^a L^{c/4-8h} \mathcal{A}_a. \quad (88)$$

The normalization  $\tilde{\mathcal{N}}^a$  can be written in terms of OPE constants, and its value will be fixed later. We turn then our attention to the computation of the conformal blocks  $\mathcal{F}_{1,1;1,1}^a$  present in the expression of the amplitudes of eq. (47). This is a standard exercise [18]. From the null state condition at level 2, the function  $\mathcal{G}^a$ ,

$$\mathcal{G}^a(\zeta) := (\zeta(1-\zeta))^{4h/3} \mathcal{F}_{1,1;1,1}^a(\zeta), \quad (89)$$

satisfies the hypergeometric equation

$$\zeta(1-\zeta)\mathcal{G}'' + \{\gamma - (1+\alpha+\beta)\zeta\}\mathcal{G}' - \alpha\beta\mathcal{G} = 0. \quad (90)$$

with parameters

$$\alpha = -4h, \beta = \frac{1}{3} - \frac{4}{3}h, \gamma = \frac{2}{3} - \frac{8}{3}h. \quad (91)$$

The roots of the indicial equation

$$r_1 = 0, \quad r_2 = 1 - \gamma, \quad (92)$$

label the two solutions of the differential equation (we take the  $\sim 0$  solutions), defining the conformal blocks of the identity  $\phi_0$ ,  $\mathcal{G}^0(\zeta)$ , and that of the operator  $\phi_2$  of weight  $h_2 = 8h/3 + 1/3$ ,  $\mathcal{G}^2(\zeta)$ :

$$\mathcal{G}^0(\zeta) = {}_2F_1 \left( \frac{1}{3} - \frac{4h}{3}, -4h; \frac{2}{3} - \frac{8h}{3}; \zeta \right) \quad (93)$$

$$\mathcal{G}^2(\zeta) = \zeta^{\frac{8h}{3} + \frac{1}{3}} {}_2F_1 \left( \frac{1}{3} - \frac{4h}{3}, \frac{4h}{3} + \frac{2}{3}; \frac{8h}{3} + \frac{4}{3}; \zeta \right). \quad (94)$$

The validity of these solutions is for  $\gamma$  not an integer.

After a little algebra the partition function reads

$$Z \left( \begin{smallmatrix} 0 & 1 \\ 1 & a \end{smallmatrix} \right) = \mathcal{N}^a L^{c/4-8h} \eta^{-c/2} \theta_3^{16h} \mathcal{G}^a(1-\zeta), \quad (95)$$

where we reabsorbed all constants in the definition of  $\mathcal{N}^a$ . The relevant  $F$ -matrices for the conformal blocks involved can be computed using standard hypergeometric identities relating the conformal blocks of the correlator  $\langle \phi_1 \phi_i \phi_j \phi_k \rangle$ , allowing explicit checks that they behave as expected under modular inversion. We report here for future convenience the  $F$ -matrices  $F_{ij} := F_{ij} \begin{bmatrix} 1/2 & 1/2 \\ 1/2 & 1/2 \end{bmatrix}$ :

$$\begin{pmatrix} F_{00} & F_{02} \\ F_{20} & F_{22} \end{pmatrix} = \begin{pmatrix} \frac{1}{\beta} & \frac{\Gamma(-\frac{8h}{3}-\frac{1}{3})\Gamma(\frac{2}{3}-\frac{8h}{3})}{\Gamma(\frac{1}{3}-\frac{4h}{3})\Gamma(-4h)} \\ \frac{\Gamma(\frac{8h}{3}+\frac{1}{3})\Gamma(\frac{8h}{3}+\frac{4}{3})}{\Gamma(\frac{4h}{3}+\frac{2}{3})\Gamma(4h+1)} & -\frac{1}{\beta} \end{pmatrix}, \quad (96)$$

where we defined  $\beta = 2 \sin(\pi(8h+1)/6) = 2 \cos(\pi/(p+1))$ , if we parametrize as usual  $c = 1 - 6/(p(p+1))$ , and  $h = h_{1,2}$ .  $\beta$  will play the role of the weight of loops in the study of loop models in the next sections.

A small- $q$  expansion of the amplitudes  $\mathcal{A}_a$  can also be computed using the explicit expression of the associated boundary states (see Appendix B). To first order we have

$$\mathcal{A}^0(\tau) = 4^{-4h_1} q^{-c/48} \left( 1 + \frac{(3-7p)^2(-2+p)}{2p(1+p)(3+p)} q + \dots \right) \quad (97)$$

$$\mathcal{A}^1(\tau) = 4^{2h_2-4h_1} q^{-c/48+h_2/2} \left( 1 + \left( \frac{9}{2} - \frac{3}{p} - \frac{45}{1+p} + \frac{80}{1+3p} \right) q + \dots \right). \quad (98)$$

We checked agreement with the expansion of eq. (95) up to order  $\hat{q}^{10}$ .

Finally, to interpret the partition function above as that of the Potts model, we fix the normalization following [11], demanding that in the limit  $\zeta \rightarrow 0$  of an infinitely long rectangle, the normalized conformal blocks<sup>2</sup> behave as

$$\mathcal{N}^a \mathcal{G}^a(1-\zeta) = 1 + O(\zeta). \quad (99)$$

This holds because for a very long rectangle, one has in both cases  $a = 0$ ,  $a = 2$ , the partition function of an horizontal strip with free boundary conditions on the sides. Both

---

<sup>2</sup> Redefining  $\phi_i^{ab} \rightarrow \lambda_i^{ab} \phi_i^{ab}$  and  $|0\rangle \rightarrow \alpha|0\rangle$  we can fix opportunely say  $\lambda_{1/2}^{0,1/2}$  and  $\lambda_{1/2}^{1,1/2}$  so that the OPE structure constants give the behavior of eq. (99).

conformal blocks should give one in that limit. We have:

$$\mathcal{N}^0 = \frac{1}{F_{00}} = \beta \quad (100)$$

$$\mathcal{N}^2 = \frac{1}{F_{20}} = \frac{\Gamma\left(\frac{4h}{3} + \frac{2}{3}\right) \Gamma(4h + 1)}{\Gamma\left(\frac{8h}{3} + \frac{1}{3}\right) \Gamma\left(\frac{8h}{3} + \frac{4}{3}\right)}. \quad (101)$$

## 4 The case of free theories

We focus now on the description of rectangular amplitudes in free theories. This section completes the discussion of free theories presented in [3] with examples with different boundary conditions along the rectangle.

### 4.1 The Laplacian of the rectangle

We start our discussion of free theories by computing the partition function of (unrooted) spanning trees on a rectangle. This problem is described by a free fermionic field theory via the matrix-tree theorem, stating that the number of spanning trees on a graph  $G$  is given by the determinant of a minor of the Laplacian matrix  $\Delta$  of  $G$  (see e.g. the review [35]):

$$Z_G^{\text{tree}} = \det(\Delta_{\setminus i}). \quad (102)$$

where  $\Delta_{\setminus i}$  is the matrix obtained from  $\Delta$  by deleting the  $i$ th row and column, to eliminate the zero eigenvalue. Then the number of spanning trees is given by a two point function in the fermionic theory. Neumann boundary conditions ( $N$ ) for the field translate to free for the spanning trees, while Dirichlet ones ( $D$ ) impose that boundary sites are linked to a single external vertex (“wired” boundary conditions).

We would like now to compute the Laplacian with either  $N$  or  $D$  on the sides of a rectangle and take the continuum limit. This can be done by taking the tensor product of Laplacians on a segment, and from that one can extract the expressions for the universal part in the limit of infinite rectangle with fixed  $\tau = iL'/L$ . Some of these results were

first given in [16] and one finds:

$$\begin{array}{c} D \\ \uparrow \\ D \end{array} = \begin{array}{c} N \\ \uparrow \\ N \end{array} = \frac{\eta(\tau)}{\sqrt{L}} \quad (103)$$

$$\begin{array}{c} N \\ \uparrow \\ D \end{array} \propto \sqrt{L} \eta(\tau) \quad (104)$$

$$\begin{array}{c} D \\ \uparrow \\ D \end{array} = \begin{array}{c} N \\ \uparrow \\ N \end{array} \propto \frac{\eta(\tau/2)}{\eta(\tau)} \quad (105)$$

$$\begin{array}{c} D \\ \uparrow \\ N \end{array} \propto \frac{\eta^2(\tau)}{\eta(\tau/2)\eta(2\tau)}. \quad (106)$$

In these results we did not keep track of proportionality coefficients, which are related to the OPE structure constants, and in principle different in each case<sup>3</sup>. The partition functions above are enough to determine all the other obtained by permuting boundary conditions. This is possible using the symmetry of describing the same partition function choosing imaginary time flowing either bottom-top or left-right (crossing symmetry of correlators of boundary fields), and modular covariance of these partition functions. For example from modular inversion one has:

$$\begin{array}{c} N \\ \uparrow \\ D \end{array} \propto \frac{\eta(2\tau)}{\eta(\tau)}, \quad (107)$$

where we have used identities listed in Appendix A. Note in particular that the partition functions (103) and (106) are modular invariant. The most important physical feature exhibited by (103)-(106) is the dimension-full factor  $L^w$ , with  $w$  the modular weight given by eq. (32). Indeed in the continuum the fermionic theory describing spanning trees is the logarithmic CFT of symplectic fermions with  $c = -2$ , where the twist field changing boundary conditions  $N$  to  $D$  and vice versa, has conformal dimension  $h_{1,2} = -1/8$  [25].

Having discussed the case of  $c = -2$  one can immediately find the result for  $c = 1$ , the free boson, by taking the power  $-1/2$  of the results above since the twist field in this case has dimension  $1/16 = (-1/2)(-1/8)$ . The case of a free boson on a rectangle was discussed in detail in [22], and our results are in agreement with those findings. Further, in that work the authors discussed also the boundary states associated to different choices of boundary conditions. The results resemble those for the cylinder boundary states except that, as expected from the general discussion of section 2, for the rectangle only

---

<sup>3</sup> Moreover the free energies computed from the lattice Laplacian contain also an additional geometry-independent constant, which we cannot predict using CFT. For example in the case of  $D$  boundary conditions around the rectangle it is [16]  $F_0 = \frac{1}{2} \log(4\sqrt{2})$ . For a recent discussion of this issue in the case of the Ising model with free boundary conditions, see [36].

one set of oscillator modes  $a_n$  of the bosonic field is left. The boundary state describing the bottom of the rectangle is [22]

$$|B_{\epsilon_l, \epsilon_r}^{\epsilon_b}\rangle = \exp\left(-\epsilon_l \epsilon_b \sum_{n>0} \frac{1}{2n} a_n^2\right) |\theta_{\epsilon_l, \epsilon_r}^{\epsilon_b}\rangle, \quad (108)$$

where  $\epsilon_{l,r,b}$  equal to  $+1$  ( $-1$ ) means  $N$  ( $D$ ) boundary conditions at left, right and bottom side respectively, and  $|\theta_{\epsilon_l, \epsilon_r}^{\epsilon_b}\rangle$  is the zero mode, which is the simple Fock vacuum except when  $\epsilon_l = \epsilon_r = +1$ , in which case is  $|p=0\rangle$  for  $\epsilon_b = 1$  and  $|x=x_0\rangle$  for  $\epsilon_b = -1$ .

## 4.2 The Ising model

In [3, 23] the case of the Ising model with  $D$  boundary conditions on all sides of the rectangle was considered, corresponding to fixing Ising spins to the same state on the boundary. The result for the corresponding rectangle boundary state has the following coherent state form

$$|B_\psi^a\rangle = \exp\left(\sum_{0\leq m<n} G_{m,n} \psi_{-m-1/2} \psi_{-n-1/2}\right) |O\rangle, \quad (109)$$

with  $|O\rangle$  the vacuum annihilated by the positive modes of the Neveu-Schwartz fermions,  $\psi_{p+1/2}|O\rangle = 0, p \in \mathbb{Z}_{\geq 0}$ , and  $G_{m,n}$  defined by

$$G(z_1, z_2) = \frac{1}{2(z_2 - z_1)} \left( \frac{\sqrt{1 - \frac{1}{z_1^2}} \sqrt{1 - \frac{1}{z_2^2}}}{1 - \frac{1}{z_1 z_2}} - 1 \right) = \frac{1}{2z_1 z_2} \sum_{m,n=0}^{\infty} \frac{G_{mn}}{z_1^m z_2^n}. \quad (110)$$

Here we will generalize this result to the case of different boundary conditions on the sides of the rectangle. This will be done by mapping correlators from the region with corners to the upper half plane, through the conformal map  $f(z) = (z + z^{-1})/2$ , similar to the situation of figure 4.

Let us consider first the upper half plane  $\mathbb{H}$  with boundary conditions for Ising spins free  $f$  on  $\{x < 1\} \cup \{x > 1\}$  and fixed (say  $+$ ) in between. This corresponds to inserting a BCC operator  $\sigma^{f,+}$  at  $x = \pm 1$ . From the fusion rules of these BCC operators

$$\sigma^{f,+} \otimes \sigma^{+,f} = I^{f,f} + \psi^{f,f}, \quad (111)$$

we know that the corresponding rectangle boundary state  $|B_{ff}^+\rangle$  is composed by two basis states, one in the sector of the identity  $|\sigma^I_\sigma\rangle$  and one in that of the energy  $|\sigma^\psi_\sigma\rangle$ :

$$|B_{ff}^+\rangle \propto |\sigma^I_\sigma\rangle + C |\sigma^\psi_\sigma\rangle. \quad (112)$$

The numerical value of  $C$  is

$$C = \frac{C_{\sigma,\sigma,\psi}^{f,+,f} \sqrt{C_{\sigma,\sigma,I}^{f,f,f}}}{C_{\sigma,\sigma,I}^{f,+,f} \sqrt{C_{I,I,I}^{f,f,f}}} = 4^{-h_\psi} \sqrt{2}, \quad (113)$$

as follows from using  $F$ -matrices for the Ising model (see e. g. [28]) after identification of boundary conditions with Virasoro representations  $f \equiv \sigma$ ,  $+$   $\equiv I$  and normalizing two point functions to one.

In order to evaluate the first contribution  $|\sigma^I_\sigma\rangle$  to the boundary state  $|B_{ff}^+\rangle$  we consider the two point correlation function of fermions in the upper half plane with these boundary conditions (see e. g. [1], eq. (22))

$$\langle \psi(w_1) \psi(w_2) \rangle_{f+f, \mathbb{H}} = \frac{1}{2(w_1 - w_2)} \left[ \left( \frac{1+w_1}{1+w_2} \right)^{1/2} \left( \frac{1-w_2}{1-w_1} \right)^{1/2} + \left( \frac{1+w_2}{1+w_1} \right)^{1/2} \left( \frac{1-w_1}{1-w_2} \right)^{1/2} \right] \quad (114)$$

where we obtained this result from the chiral correlator  $\langle \psi(w_1) \psi(w_2) \sigma(1) \sigma(-1) \rangle$  and omitting irrelevant factors. This result can be related to the boundary state  $|B_{ff}^+\rangle$  describing the geometry  $\mathcal{D}$  with  $f+f$  boundary conditions through

$$\langle \psi(z_1) \psi(z_2) \rangle_{f+f, \mathcal{D}} = \langle O | \psi(z_1) \psi(z_2) | B_{ff}^+ \rangle = \left( \frac{\partial w_1}{\partial z_1} \frac{\partial w_2}{\partial z_2} \right)^{1/2} \langle \psi(w_1) \psi(w_2) \rangle_{f+f, \mathbb{H}}. \quad (115)$$

Following the discussion in [3], we look for a fermionic coherent state form of the boundary state

$$|\sigma^I_\sigma\rangle = 4^{-2h_\sigma} : \exp \left( \oint \frac{dz}{2i\pi} \oint \frac{dz'}{2i\pi} \psi(z) G(z, z') \psi(z') \right) : |O\rangle, \quad (116)$$

where the factor  $4^{-2h_\sigma}$  is introduced in order to obtain consistency with the definition of basis states (17). Substituting this in equation (115) one can easily determine the function  $G(z, z')$ . It is convenient to split expression (114) into the sum of two terms. Going through the calculations leads to the introduction of two functions

$$G^{(1)} = \frac{1}{4(z_2 - z_1)} \left[ \frac{\sqrt{1 - \frac{1}{z_1^2}} \sqrt{1 - \frac{1}{z_2^2}}}{1 - \frac{1}{z_1 z_2}} \frac{(1 + \frac{1}{z_1})(1 - \frac{1}{z_2})}{(1 - \frac{1}{z_1})(1 + \frac{1}{z_2})} - 1 \right] \quad (117)$$

and

$$G^{(2)} = \frac{1}{4(z_2 - z_1)} \left[ \frac{\sqrt{1 - \frac{1}{z_1^2}} \sqrt{1 - \frac{1}{z_2^2}}}{1 - \frac{1}{z_1 z_2}} \frac{(1 - \frac{1}{z_1})(1 + \frac{1}{z_2})}{(1 + \frac{1}{z_1})(1 - \frac{1}{z_2})} - 1 \right] \quad (118)$$

for which we define the expansions

$$G^{(i)} = \frac{1}{2z_1 z_2} \sum_{m,n=0}^{\infty} \frac{G_{mn}^{(i)}}{z_1^m z_2^n} \quad (119)$$

so that the boundary state gathers the contribution

$$|_{\sigma}^I \rangle = 4^{-2h_{\sigma}} \exp \left( \sum_{0 \leq m < n}^{\infty} [G_{mn}] \psi_{-m-1/2} \psi_{-n-1/2} \right) |O\rangle \quad (120)$$

where we defined  $G = G^{(1)} + G^{(2)}$ . The first values of  $G_{mn}$  read

$$\begin{aligned} G_{01} &= -\frac{3}{2} \\ G_{03} &= -\frac{7}{8}, G_{12} = -\frac{3}{8} \\ G_{05} &= -\frac{11}{16}, G_{14} = -\frac{1}{16}, G_{23} = -\frac{7}{8} \\ G_{07} &= -\frac{75}{128}, G_{16} = -\frac{3}{128}, G_{25} = -\frac{55}{128}, G_{34} = -\frac{63}{128}. \end{aligned} \quad (121)$$

This leads to the first few terms in the expansion of the boundary state

$$|_{\sigma}^I \rangle = 4^{-2h_{\sigma}} \left[ 1 + \frac{3}{2} \psi_{-1/2} \psi_{-3/2} + \frac{7}{8} \psi_{-1/2} \psi_{-7/2} + \frac{3}{8} \psi_{-3/2} \psi_{-5/2} + \dots \right] |O\rangle. \quad (122)$$

We now determine the other contribution  $|_{\sigma}^{\psi} \rangle$  to  $|B_{ff}^+\rangle$  in addition to  $|_{\sigma}^I \rangle$ . For doing that we use now the chiral correlator  $\langle \psi(w_0) \psi(w_1) \psi(w_2) \sigma(1) \sigma(-1) \rangle$  in [1] (eq. (66) of that reference) and send  $w_0$  to infinity to obtain

$$\langle \psi(\infty) \psi(w_1) \psi(w_2) \rangle_{f+f, \mathbb{H}} = \frac{w_1^2 + w_2^2 - w_1 w_2 - 1}{(w_1 - w_2)(w_1^2 - 1)^{1/2}(w_2^2 - 1)^{1/2}}. \quad (123)$$

Setting  $u = \frac{1}{z_1}$  and  $v = \frac{1}{z_2}$ , we find the corresponding correlator in the  $z$  plane

$$\begin{aligned} \langle \psi(\infty) \psi(z_1) \psi(z_2) \rangle_{f+f, \mathcal{D}} &= \frac{(v-u)(1-uv)}{(1-u^2)^{1/2}(1-v^2)^{1/2}} \\ &+ \frac{(1-u^2)^{1/2}(1-v^2)^{1/2}}{(v-u)(1-uv)} \left[ v^2 \frac{1-u^2}{1-v^2} + u^2 \frac{1-v^2}{1-u^2} \right]. \end{aligned} \quad (124)$$

We represent this expression alternatively as

$$\langle \psi(\infty) \psi(z_1) \psi(z_2) : \exp \left( \oint \frac{dz}{2i\pi} \oint \frac{dz'}{2i\pi} \psi(z) G(z, z') \psi(z') \right) : \psi(0) |O\rangle. \quad (125)$$

This gives us the lengthy expression

$$G(z_1, z_2) = \frac{1}{2} \frac{(v-u)(1-uv)}{(1-u^2)^{1/2}(1-v^2)^{1/2}} + \frac{1}{2} \frac{(1-u^2)^{1/2}(1-v^2)^{1/2}}{(v-u)(1-uv)} \left[ v^2 \frac{1-u^2}{1-v^2} + u^2 \frac{1-v^2}{1-u^2} \right] - \frac{u^2 + v^2 - uv}{(u-v)}, \quad (126)$$

where we used that

$$\langle \psi(\infty) \psi(z_1) \psi(z_2) \psi(0) \rangle = \frac{u^2 + v^2 - uv}{v-u}. \quad (127)$$

We finally expand as before

$$G(z_1, z_2) = \frac{uv}{2} \sum_{m,n \geq 0} G_{mn} u^m v^n, \quad (128)$$

from which we get the final result

$$|_{\sigma}^{\psi} \rangle = 4^{h_{\psi}-2h_{\sigma}} \exp \left[ \sum_{0 \leq m < n} G_{mn} \psi_{-m+1/2} \psi_{-n+1/2} \right] \psi(0) |O\rangle. \quad (129)$$

In the end one gets the following expression

$$|_{\sigma}^{\psi} \rangle = 4^{h_{\psi}-2h_{\sigma}} \left[ 1 - \frac{1}{2} \psi_{1/2} \psi_{-5/2} - \frac{3}{8} \psi_{1/2} \psi_{-9/2} - \frac{5}{16} \psi_{1/2} \psi_{-13/2} - \frac{9}{8} \psi_{-3/2} \psi_{-5/2} - \frac{5}{8} \psi_{-3/2} \psi_{-9/2} + \dots \right] \psi_{-1/2} |O\rangle, \quad (130)$$

for the second (odd) contribution to the boundary state.

Taking overlap of these boundary states we can compute partition functions with different boundary conditions of Ising spins, and their agreement with four point functions of BCC operators along the general scheme of section 3, can be readily checked. We will not present here the details of this check, but support our results with lattice computations for the Ising model instead.

#### 4.2.1 Lattice Ising model

In this section we will compute the scalar products of the discretization of the boundary state  $|B_{ff}^+\rangle$  with excited states in the Ising Hamiltonian. We consider the Hamiltonian limit of the 2D critical Ising model on a strip with free/free boundary conditions:

$$H = -\frac{1}{2} \left( \sum_{i=1}^L \sigma_i^z + \sum_{i=1}^{L-1} \sigma_i^x \sigma_{i+1}^x \right). \quad (131)$$



Now recall that the Hamiltonian (131) is related to the 2D Ising model in the  $\sigma^x$  basis. Then to make the contact with the 2D model, we should rotate 90 degrees clockwise the spins of the chain in the  $x - z$  plane, that is, we define the “fixed” boundary state  $|B_{ff}^+\rangle_L$  as

$$|B_{ff}^+\rangle_L = |\rightarrow \cdots \rightarrow\rangle = \frac{1}{\sqrt{2^L}} \sum_{\{\mu_i^z = \uparrow, \downarrow\}} |\mu_1^z \cdots \mu_L^z\rangle. \quad (132)$$

We diagonalize the chain [29] to obtain the eigenvectors  $|k\rangle_L$ , and compute numerically the scalar products  ${}_L\langle B_{ff}^+ | k \rangle_L$ . This task is simplified by using the free fermionic nature of the problem, in a way similar to what we did for free boundary conditions in [3]. This time, however, the computations are more complex and we have restricted the analysis to small system sizes (up to  $L = 30$  sites). Before presenting the results, we recall that due to the anomaly at the corners (see eq. (32)), scalar products between a lattice rectangular boundary state  $|B\rangle_L$  and the (normalized)  $k$ -th excited state  $|k\rangle_L$  of the strip Hamiltonian, are expected to scale as [3]:

$$-\log({}_L\langle B | k \rangle_L) = a_0 L + a_1 \log L + a_2 + \frac{a_3}{L} + \frac{a_4}{L^2} + O\left(\frac{1}{L^3}\right), \quad (133)$$

with

$$a_1 = 2(h_l + h_r) - \frac{c}{8}. \quad (134)$$

The value of the CFT scalar product  $\langle B | k \rangle$  is then extracted from

$$a_2 = \gamma - \log(\langle B | k \rangle), \quad (135)$$

$\gamma$  determined normalizing  $\langle B | 0 \rangle = 1$ . See section 5.2 below for a systematic study of these coefficients. For computing  $\langle B | k \rangle$ , we actually fit

$$-\log\left(\frac{{}_L\langle B | k \rangle_L}{{}_L\langle B | 0 \rangle_L}\right) = a_2 + \frac{a_3}{L} + \frac{a_4}{L^2} + \frac{a_5}{L^3}. \quad (136)$$

We present the data obtained in table 1. The value  $a_1 = 2 \times 2/16 - 1/16 = 3/16$  is found with good accuracy only for the first lower excited states. The continuum limit of the excited states of the chain is associated to a CFT state obtained by the action of negative fermionic modes on the vacuum. It is important to distinguish the two sectors, even and odd number of fermions, corresponding respectively to descendants of the identity  $I$  and of the energy  $\psi$  in the CFT. We replace  $\gamma$  in (135) by  $\gamma + \tilde{\gamma}$  if  $|k\rangle$  is a descendant of  $\psi$ .  $\tilde{\gamma}$  is written as minus the logarithm of a prefactor  $\tilde{C}$  multiplying the states in the sector of  $\psi$ . Looking at  $\langle B_{ff}^+ | 1 \rangle$  (where  $|1\rangle = \psi_{-1/2}|0\rangle$ ) determines

$$\tilde{C} = 1.41422 \pm 0.00002. \quad (137)$$

This agrees very well with the prediction from the general theory eq. (113) (the factor  $4^{-h_\psi}$  simplifies with  $4^{h_\psi-2h_\sigma}/4^{-2h_\sigma}$  from the normalization of the basis states  $|\sigma^\psi_\sigma\rangle$  and  $|\sigma^I_\sigma\rangle$ ), providing a lattice measurement of boundary OPE coefficients. In table 1 we list the scalar products obtained. The agreement with the CFT prediction is good, validating our analytical computation.

	$h_k$	numerics	CFT
$\langle B_{ff}^+ 0\rangle$	0	1	1
$\langle B_{ff}^+ 1\rangle$	1/2	1	1
$\langle B_{ff}^+ 2\rangle$	3/2	0	0
$\langle B_{ff}^+ 3\rangle$	2	$1.499999 \pm 0.000020$	$3/2 = 1.5$
$\langle B_{ff}^+ 4\rangle$	5/2	$0.500079 \pm 0.000012$	$1/2 = 0.5$
$\langle B_{ff}^+ 5\rangle$	3	0	0
$\langle B_{ff}^+ 6\rangle$	7/2	0	0
$\langle B_{ff}^+ 7\rangle$	4	$0.875178 \pm 0.000020$	$7/8 = 0.875$
$\langle B_{ff}^+ 8\rangle$	4	$0.374991 \pm 0.000005$	$3/8 = 0.375$
$\langle B_{ff}^+ 9\rangle$	9/2	$0.375315 \pm 0.000031$	$3/8 = 0.375$
$\langle B_{ff}^+ 10\rangle$	9/2	$1.125002 \pm 0.000020$	$9/8 = 1.125$

Table 1: Scalar product of  $|B_{ff}^+\rangle$  and  $|k\rangle$  from finite size scaling (numerics) and comparison with CFT prediction.  $h_k$  is the conformal dimension of the field  $|k\rangle$ . Chains of size up to  $L = 30$  sites are used.

## 5 Loop models

### 5.1 BCFT of loop models

The lattice model we consider now is the dense loop model based on the Temperley-Lieb algebra underlying the Potts model [30]. We consider a system of  $L$  (even or odd) strands, with free (reflecting) boundary conditions at both boundaries. At the critical point, the anisotropic version of the model is defined by the Hamiltonian:

$$H = - \sum_{i=0}^{L-2} e_i, \quad (138)$$

where  $e_i$  are the TL generators. This Hamiltonian acts on link states, patterns of connectivities of sites, and has a triangular block form, with  $j = 0, 2, \dots, L$  ( $L$  even) or  $j = 1, 3, \dots, L$  ( $L$  odd), the number of through lines, indexing each block [30].

The continuum limit of this loop model, when we parametrize the loop weight as  $\beta = 2 \cos(\pi/(p+1))$  ( $p \geq 1$  is a real parameter which we keep generic here), is a CFT

with central charge  $c = 1 - 6/(p(p+1))$ . The primary boundary fields of the resulting (quasi-rational) boundary CFT are  $\phi_j$ ,  $j \in \mathbb{N}$  (see e. g. [33]).  $\phi_j$  is interpreted as the operator creating  $j$  lines in the continuum limit of the loop model, and corresponds to the irreducible Virasoro representation with highest weight  $\phi_{1,1+j}$  (Kac table notation), with conformal dimension  $h_{1,1+j} = \frac{j(jp-2)}{4(p+1)}$ . The primaries  $\phi_j$  generically fuse as spin- $(j/2)$   $\text{su}(2)$  representations:

$$V_i \times V_j = \sum_{k \in \mathcal{I}} V_k, \quad \mathcal{I} = \{|i-j|, |i-j|+2, \dots, i+j\}. \quad (139)$$

The allowed boundary conditions one can put on the strip are given by the labels  $j$  of Virasoro representations. Setting  $i$  and  $j$  on the boundaries will then allow the propagation of only the sectors given by the fusion of  $i$  and  $j$  [8]. It is possible to manufacture microscopic boundary conditions for the lattice model to reproduce this behavior [32] (and see below). Note that free (reflecting) boundary conditions on the lattice, without restrictions on the number of through lines, correspond to setting on both boundaries the label  $j \rightarrow \infty$ . The BCC operator between boundaries  $j$  and  $j'$  is given by  $\phi_{|j-j'|}^{j,j'}$ , the operator of smallest conformal weight in the spectrum of the transfer matrix for a strip with  $j$  and  $j'$  on the sides. Fusion rules of these boundary operators are only a subset of those for free boundaries, eq. (139) (because some boundary OPE structure constants vanish):

$$\phi_{|i-j|}^{i,j} \times \phi_{|j-k|}^{j,k} = \sum_{s \in \mathcal{I}'} \phi_s^{i,k}. \quad (140)$$

where  $\mathcal{I}' = (\{|i-k|, |i-k|+2, \dots, i+k\} \cap \{||i-j|-|j-k||, ||i-j|-|j-k||+2, \dots, |i-j|+|j-k|\})$ . This restriction comes from the compatibility of the number of lines inserted by the fields in the corners and that which is allowed by the boundary conditions. We depict in figure 6 the geometric interpretation of the two-point function of BCC operators as the contraction of  $|i-j|$  lines originating from the point in which the boundary condition is changed from  $i$  to  $j$  and terminating at the point in which we change from  $j$  to  $i$ . More details about this geometric interpretation of the fields will be given in the next section, where we also present numerical checks.



We support our claim with the numerical results (labeled num) of table 2, obtained for fugacity of loops  $\beta = \sqrt{2}$  and to be compared with the CFT results (labeled theo), corresponding to central charge  $c = 1/2$ . Denote by  $|k\rangle_L$  the  $k$ -th eigenvector (normalized according to the loop scalar product) of the Hamiltonian restricted to the sector with  $s$  through lines. As discussed above, the scalar product of a rectangular boundary state and  $|k\rangle_L$  has the form (133), and now  $\gamma = -\log(\tilde{\alpha})$ ,  $\tilde{\alpha} := \alpha 4^{h_s - h_i - h_j}$ , see eq. (17). In the data presented below  $\tilde{\alpha}$  is determined by giving the expected value of  $a_1$  ( $a_1$  theo) as input in the fit.

The scaling limit  $|k\rangle$  of  $|k\rangle_L$  used to determine  $\langle B|k\rangle$  (theo), are for generic  $k$  given by a combination of Virasoro descendants at a level determined by the energy of  $|k\rangle$ . The state  $|0\rangle$  is clearly identified with the primary  $|\phi_j\rangle$  for each sector. Then recall that the continuum theory has field content given generically by the quotient of Virasoro Verma modules  $V_{1,1+s}/V_{1,-1-s}$  (with the usual Kac table notation for Verma modules) [33]. In the sector  $s = 0$ , we identify then (due to normalization)  $|1\rangle = \sqrt{2/c}L_{-2}|0\rangle$ ,  $|2\rangle = \sqrt{1/2c}L_{-3}|0\rangle$ . When  $s = 1$ , we have  $|1\rangle = 1/\sqrt{2h_1}L_{-1}|\phi_1\rangle$ ,  $|2\rangle = 1/\sqrt{4h_1 + c/2}L_{-2}|\phi_1\rangle$ . For  $s = 2$ ,  $|1\rangle = 1/\sqrt{2h_2}L_{-1}|\phi_2\rangle$ , and  $|2\rangle = 2/3L_{-2}|\phi_2\rangle$  at  $c = 1/2$  (note that this last is a priori an unknown combination of Virasoro descendants at level two, which for  $c = 1/2$  is fixed using that  $|\phi_2\rangle$  is also degenerate at level two, since  $h_{1,3} = h_{2,1}$ ). Scalar products  $\langle B|k\rangle$  (theo) in table 2 are then computed using the above formulas for  $|k\rangle$ 's and the explicit form of  $|B\rangle$ 's, eq. (17) (see Appendix B for  $|1^0_1\rangle$ ,  $|1^2_1\rangle$  and eq.(86) for  $|0^1_1\rangle$  and  $|2^2_0\rangle$ ), specialized at  $p = 3$ .

$ B\rangle_L$	$a_1$ num	$a_1$ theo	$\tilde{\alpha}_{ij}^s$	$\langle B 1\rangle$ num	$\langle B 1\rangle$ theo	$\langle B 2\rangle$ num	$\langle B 2\rangle$ theo
$ 1^0_1\rangle_L$	0.18712(307)	0.1875	1.27053(16)	1.50004(21)	1.5	0	0
$ 0^1_1\rangle_L$	0.06278(131)	0.0625	1.08322(6)	0.70704(5)	$\simeq 0.70711$	0.35360(3)	$\simeq 0.35355$
$ 2^2_0\rangle_L$	0.93778(865)	0.9375	4.33940(152)	2.00057(74)	-2	2.50616(105)	2.5
$ 1^2_1\rangle_L$	0.18938(76)	0.1875	1.79691(8)	0	0	0.50115(15)	0.5

Table 2: Lattice scalar products for loop fugacity  $\beta = \sqrt{2}$  and comparison with the results for the  $c = 1/2$  CFT. Extrapolations are determined by fitting values for  $L = 10 \rightarrow 24$ .  $\tilde{\alpha}_{ij}^s = \alpha_{ij}^s 4^{h_s - h_i - h_j}$ .

Finally, we note that the state defined in (141) is of course not the only microscopic state giving rise to  $|i^s_j\rangle$  in the continuum limit. Any similar state obtained via local modifications (e. g. by allowing a finite number of arches between the through lines, etc.) would obey the same property, albeit with a different value of the coefficient  $\alpha_{ij}^s$ .

### 5.3 Geometric interpretation of conformal blocks

Up to now we have given numerical support to our claim that the rectangle basis states  $|_{i,j}^{s,j}\rangle$  defined in eq. (17) can be interpreted as the continuum limit of microscopic boundary states with a given pattern of connectivities. Here we want to push this discussion further and associate a geometric picture in terms of loop configurations to conformal blocks building the correlator of BCC operators. According to the previous discussion, we have the identification:

$${}_L\langle_{s}^{i,l}|T^{L'}|_j^s{}_k\rangle_L \xrightarrow{(\text{FP})} \alpha_{jk}^s \alpha_{il}^s \mathcal{A}_s^{i,j,k,l}(\tau). \quad (144)$$

We depict in figure 7 two configurations contributing to the lattice amplitude  ${}_L\langle_{2}^{2,2}|T^{L'}|_2^2{}_2\rangle_L$  and one to the amplitude  ${}_L\langle_{4}^{2,2}|T^{L'}|_2^4{}_2\rangle_L$ , drawing only lines inserted at the corners.

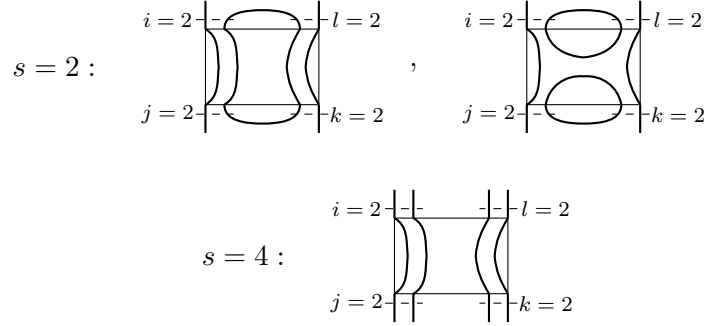


Figure 7: Configurations contributing to the lattice amplitudes  ${}_L\langle_{s}^{2,2}|T^{L'}|_2^s{}_2\rangle_L$  for  $s = 2, 4$ .

We see that  $\mathcal{A}_s^{i,j,k,l}(\tau)$  is then associated to the continuum limit of lattice amplitudes where we insert  $i$  lines in top left corner,  $l$  in top right,  $j$  in the bottom left and  $k$  in bottom right.  $s$  of the lines (the most exterior ones) are forced to propagate. The other lines can—but are not obliged to—be contracted. Only if  $s = i + l = j + k$  ( $s = 4$  in the example of figure 7), the amplitude is associated to configurations where all lines inserted at the corners are forced to propagate. For example, the CFT partition function of figure 2 will be  $Z(0_{i+j}^i) \propto L^w \mathcal{A}_{i+j}^{i,i,j,j}$ . The only term in the amplitude sensible to the changing of the number of through lines (associated to different fusion sectors) is the conformal block. Then we are led to the geometrical identification of conformal blocks which we schematically represent as

$$\mathcal{F}_{il;jk}^s(1-\zeta) \longleftrightarrow \begin{array}{c} \square \\ \text{with a central circle and lines connecting the corners to the circle} \end{array}$$

where the diagram on the right has a fixed number  $s$  of through lines and the bubble stays for the possibility of contracting or not the other lines inserted at the corner.

We recall that in general the partition function  $Z$  is given by a sum of amplitudes from the relation (31), and its geometric interpretation follows from that of the amplitude. We will comment more on that in section 5.5, where we discuss the universal character of the coefficients  $\alpha_{ij}^s$ , and the precise relations between lattice amplitudes and CFT partition functions (30).

### 5.3.1 Probabilistic interpretation

We can easily obtain interesting results from the discussion above as follows. We specialize to the case of one line insertion at every corner,  $i = j = k = l = 1$ . In this case, the amplitudes are formally equivalent to that for the Potts model with insertions of  $\phi_{1,2}^{f,F}$  changing from free  $f$  boundary conditions to fixed  $F$ , and were computed explicitly in section 3.2.2. The partition function

$$Z \left( \begin{smallmatrix} 1 & 1 \\ 0 & 1 \end{smallmatrix} \right) (\tau) = \mathcal{N}^2 \eta^{-c/2}(\tau) \theta_3^{16h}(\tau) \mathcal{G}^2(1 - \zeta) \propto L^w \mathcal{A}_2(\tau)$$

is unambiguously the (universal part of the) continuum limit of a loop model where the two lines inserted at left and right bottom corners constrained to propagate in the vertical direction. Consequently

$$Z \left( \begin{smallmatrix} 0 & 1 \\ 1 & 1 \end{smallmatrix} \right) (\tau) = \mathcal{N}^2 L^w \eta^{-c/2}(\tau) \theta_3^{16h}(\tau) \mathcal{G}^2(\zeta(\tau)) \propto (L')^w \mathcal{A}_2(-1/\tau),$$

is then the partition function of a loop model with the two lines inserted at left bottom and left top corners constrained to propagate in the horizontal direction. Then one can interpret the conformal blocks  $\mathcal{G}^a$  as in the top of figure 8. The geometric interpretation of every other amplitude involving boundary states with  $\phi_1$  insertions at the corner will follow from the decomposition in terms of  $\mathcal{A}_2(\tau)$  and  $\mathcal{A}_2(-1/\tau)$ . For example for  $\mathcal{A}_0(\tau)$ , we can use the hypergeometric identity  $\mathcal{G}^0(1 - \zeta) = 1/F_{20} \mathcal{G}^2(\zeta) - F_{22}/F_{20} \mathcal{G}^2(1 - \zeta) \propto \mathcal{G}^2(\zeta) + 1/\beta \mathcal{G}^2(1 - \zeta)$ , see the bottom of figure 8.

We have seen that the two elementary events which can happen when inserting a line in each corner are described by  $\mathcal{G}^2(1 - \zeta)$  and  $\mathcal{G}^2(\zeta)$ . Then, the probability of having these two lines flowing vertically is:

$$P(\tau) = \frac{\begin{array}{c} \square \quad \square \\ \hline \end{array}}{\begin{array}{c} \square \quad \square \\ \hline \end{array} + \begin{array}{c} \square \quad \square \\ \hline \end{array}} = \frac{Z \left( \begin{smallmatrix} 1 & 1 \\ 0 & 1 \end{smallmatrix} \right) (\tau)}{Z \left( \begin{smallmatrix} 1 & 1 \\ 0 & 1 \end{smallmatrix} \right) (\tau) + Z \left( \begin{smallmatrix} 0 & 1 \\ 1 & 1 \end{smallmatrix} \right) (\tau)} = \frac{\mathcal{G}^1(1 - \zeta)}{\mathcal{G}^1(1 - \zeta) + \mathcal{G}^1(\zeta)} \quad (145)$$

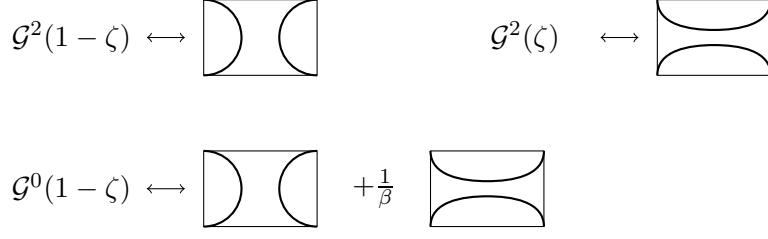


Figure 8: Geometric interpretation of the conformal block  $\mathcal{G}^2$  and  $\mathcal{G}^0$ . Thick lines represent the non-contractible lines created by the one-leg operators in the corners propagating or not through the system (time is flowing upwards).

The probability that the lines propagate horizontally is clearly  $1 - P(\tau)$ . Note that whatever normalization of the partition function drops out since it is common to both partition functions.

We first consider the case of percolation, for which  $\beta = 1$ , corresponding to  $c = h = 0$ . We have:

$$P_{c=0, \text{dense}}(\zeta) = \frac{(1 - \zeta)^{\frac{1}{3}} {}_2F_1\left(\frac{1}{3}, \frac{2}{3}; \frac{4}{3}; 1 - \zeta\right)}{(1 - \zeta)^{\frac{1}{3}} {}_2F_1\left(\frac{1}{3}, \frac{2}{3}; \frac{4}{3}; 1 - \zeta\right) + \zeta^{\frac{1}{3}} {}_2F_1\left(\frac{1}{3}, \frac{2}{3}; \frac{4}{3}; \zeta\right)} \quad (146)$$

$$= \frac{\Gamma(\frac{2}{3})}{\Gamma(\frac{4}{3})\Gamma(\frac{1}{3})} (1 - \zeta)^{\frac{1}{3}} {}_2F_1\left(\frac{1}{3}, \frac{2}{3}; \frac{4}{3}; 1 - \zeta\right) \quad (147)$$

$$= \frac{\Gamma(\frac{2}{3})}{\Gamma(\frac{1}{3})\Gamma(\frac{4}{3})} (1 - \zeta)^{\frac{1}{3}} \left(1 - \frac{1}{6}(1 - \zeta) + \frac{5}{63}(1 - \zeta)^2 + O((1 - \zeta)^3)\right). \quad (148)$$

This quantity is precisely the crossing probability computed by Cardy in [9, 11], that is, the probability that there is at least one Fortuin-Kasteleyn (FK) crossing cluster spanning the rectangle in the vertical direction. We now comment on this relation. Microscopically, the configurations of loops contributing to the numerator of our formula are those where the two lines inserted at the corners propagate from bottom to top. In terms of FK clusters (which are encircled by the loops), this corresponds to counting cluster configurations with “wired” boundary conditions on top and bottom rows, and to the constraint that there is at least one spanning cluster crossing the rectangle, see figure 9. Call such ensemble of cluster configurations  $\mathcal{S}_w$ .

Instead the configurations counted by Cardy’s formula, which we denote by  $\mathcal{S}$ , are simply those with at least one spanning cluster, without imposing wired boundary conditions. We now show that

$$\#(\mathcal{S}) = 2^L \times 2^L \times \#(\mathcal{S}_w), \quad (149)$$



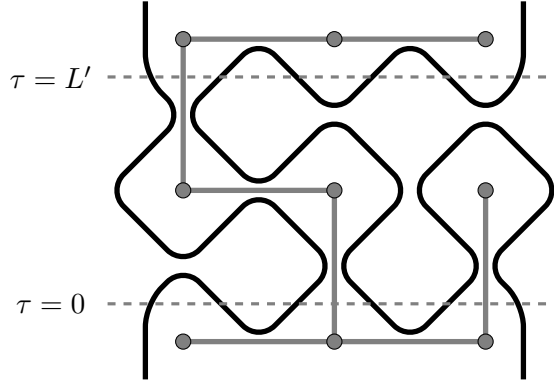


Figure 9: A configuration of loops (black) and the corresponding configuration of Fortuin-Kasteleyn clusters (gray). The through lines inserted at the bottom corners are forced to propagate to the top, and wired boundary conditions (all bonds open) are imposed on the links of the bottom and top rows of the lattice where the Fortuin-Kasteleyn clusters live.  $\tau = 0$  and  $\tau = L'$  are initial and final discrete imaginary times of the transfer matrix evolution in the vertical direction.

where  $\#(E)$  is the number of elements of the set  $E$ . First note that changing the status (open or closed) of links in the bottom and top rows of the lattice where FK clusters live, transforms a configuration  $s \in \mathcal{S}$  into another  $s' \in \mathcal{S}$ . Then we can group the spanning configurations in classes differing by only the status of bottom and top links, and for each class we choose the representative with all the bottom and top links open. Since there are  $2^L \times 2^L$  (first factor for the possible status of top links and second for those of bottom links) elements in each class, eq. (149) follows. Now note that also the set of all possible (not only spanning) cluster configurations can be divided in classes with elements differing by the status of top and bottom links as before. Then, if we compute the crossing probability by dividing the number of spanning configurations  $\#(\mathcal{S})$  by the number of all possible configurations, the multiplicative factor  $2^L \times 2^L$  drops out, and the equality of our formula with Cardy's one is established. The above argument does not work anymore when we have generic weight of clusters  $\beta$ , since spanning configurations cannot be regrouped then due to the different powers of  $\beta$  weighting each configuration. Crossing probabilities for generic fugacity  $\beta$  have been computed using SLE methods, see [2].

#### 5.4 Logarithmic cases

We have anticipated in section 3.2.2 that for certain (logarithmic) values of the central charge the conformal blocks for  $\phi_1$  insertions at the corners, (93)-(94), are ill-defined.

Indeed, more fundamentally fusion of the fields at these points cannot be decomposed onto irreducible Virasoro modules [20, 21]. For the operators degenerate at level two we are considering, this happens for  $c = -2$  and  $\phi_1 = \phi_{1,2}$   $h = -1/8$  (dense polymers), and for  $c = 0$  and  $\phi_1 = \phi_{2,1}$ ,  $h = 5/8$  (dilute polymers). In these cases, we have the following behavior of conformal blocks ( $\epsilon = p - 1$  in (150),  $\epsilon = p - 2$  in (151), where we parametrized  $c = 1 - 6/(p(p + 1))$ )

$$\lim_{\epsilon \rightarrow 0} \mathcal{G}^0(\zeta) = \frac{2}{\pi} K(\zeta); \quad \lim_{\epsilon \rightarrow 0} \mathcal{G}^2(\zeta) = \frac{2}{\pi} K(\zeta); \quad (150)$$

$$\mathcal{G}^0(\zeta) = \frac{15}{16\epsilon} S_2(\zeta) + O(\epsilon); \quad \lim_{\epsilon \rightarrow 0} \mathcal{G}^2(\zeta) = S_2(\zeta). \quad (151)$$

$K$  is the complete elliptic integral of the first kind of parameter  $\zeta$  and

$$S_2(\zeta) := \zeta^2 {}_2F_1\left(-\frac{1}{2}, \frac{3}{2}; 3; \zeta\right). \quad (152)$$

For dense polymers the degeneracy  $\mathcal{G}^0(\zeta) \rightarrow \mathcal{G}^2(\zeta)$  arises because the roots of the indicial equation (92) coincide, so that one has to replace one conformal block with the missing solution of the differential equation which generally is given by a derivation procedure w.r.t. the root, and here can be written as ( $\epsilon = p - 1$ )

$$\lim_{\epsilon \rightarrow 0} \frac{\mathcal{G}^2(\zeta) - \mathcal{G}^0(\zeta)}{\epsilon} \propto K(1 - \zeta) - \frac{\log(16)}{\pi} K(\zeta). \quad (153)$$

In terms of fusion rules this is stated as the degeneracy of the two fields  $\phi_0$  and  $\phi_2$ , which are replaced by the identity and its logarithmic partner under the Virasoro algebra [20]. For dilute polymers,  $\mathcal{G}^0$  here has to be replaced by the logarithmic conformal block, which can be written as ( $\epsilon = p - 2$ )

$$\lim_{\epsilon \rightarrow 0} \frac{1}{F_{02}} (\mathcal{G}^0(\zeta) - F_{00} \mathcal{G}^0(1 - \zeta)) = (1 - \zeta)^2 {}_2F_1\left(-\frac{1}{2}, \frac{3}{2}; 3; 1 - \zeta\right) \quad (154)$$

$$= S_2(1 - \zeta), \quad (155)$$

where  $F_{ij}$  are the fusing matrices of four  $\phi_1$  fields at generic central charge, eq. (96). Again this is stated as the degeneracy of the stress tensor and the field  $\phi_2$ , which are organized in an indecomposable module under the Virasoro algebra [21].

The presence of a divergence is clearly a difficulty for the interpretation of the partition function as that of a statistical model. We consider the partition functions  $Z\left(0 \frac{1}{1} a\right)$ ,  $a = 0, 2$  computed in section 3.2.2, for which we have the geometrical interpretation discussed in the previous section. In particular recall that  $Z\left(0 \frac{1}{1} 2\right)$  is given by configurations of loops where we constrain the two lines inserted at the bottom corners to

propagate without being contracted. We assume now that the geometric interpretation of boundary states goes through also in the dilute case, where the value of  $h$  in the formulas is  $h_{2,1}$ . We expect physically that these partition functions should be well defined for every value of loop fugacity  $\beta$ , also at  $\beta = 0$ , which is the case we are after for polymers. The solution to this is simply hidden in the normalization of the partition function, eq. (95). In the case of dense polymers  $\mathcal{N}^0 = \mathcal{N}^2 = 0$ . This does not come as a surprise, and should be traced back to the presence of a single loop on the rectangle. Factorizing this trivial zero, one then gets that for dense polymers:

$$Z \left( \begin{smallmatrix} 1 & \\ 0 & 1 \end{smallmatrix} \middle| 2 \right) (h = -1/8) = Z \left( \begin{smallmatrix} 1 & \\ 0 & 1 \end{smallmatrix} \middle| 0 \right) (h = -1/8) = \sqrt{L}\eta\theta_3^{-2} \frac{2}{\pi} K(1 - \zeta) \quad (156)$$

$$= \sqrt{L}\eta, \quad (157)$$

where we used the identity  $2K(1 - \zeta(\tau)) = \pi\theta_3(\tau)^2$ . As a highly not-trivial check of the above result we can compare with the expression coming from the determinant of the Laplacian with different boundary conditions on opposite edges, see eq. (104).

For dilute polymers one has

$$\mathcal{N}^0 \rightarrow \frac{\pi}{2}\epsilon + O(\epsilon^2) \quad (158)$$

$$\mathcal{N}^1 \rightarrow \frac{15}{32}\pi + O(\epsilon). \quad (159)$$

Note that the indecomposability parameter  $b = 5/6$  [21], characterizing the Jordan cell of the stress tensor for dilute polymers, is present explicitly in the coefficients,  $h^2/b = 15/32$ . Finally we predict again degeneracy of both partition functions

$$Z \left( \begin{smallmatrix} 1 & \\ 0 & 1 \end{smallmatrix} \middle| 2 \right) (h = 5/8) = Z \left( \begin{smallmatrix} 1 & \\ 0 & 1 \end{smallmatrix} \middle| 0 \right) (h = 5/8) = L^{-5}\theta_3^{-10}S_2(1 - \zeta). \quad (160)$$

The degeneracy we have observed could be understood more fundamentally as the gluing of the two sectors  $\phi_0$  and  $\phi_2$  in an indecomposable module corresponding to a single boundary condition.

It is of interest now to see what is the behavior of probabilities (145) at the logarithmic points discussed above,  $c = -2$  dense and  $c = 0$  dilute. The outcome is that probabilities are well defined but their expansion shows logarithmic terms. For expanding around  $\zeta = 1$ , the case of a tall rectangle, we use

$$\mathcal{G}^2(\zeta) = F_{20}\mathcal{G}^0(1 - \zeta) + F_{22}\mathcal{G}^2(1 - \zeta). \quad (161)$$

As  $h \rightarrow -1/8$  (dense case) we see from formulas (96) that  $F_{20} \rightarrow \infty$  and  $F_{22} \rightarrow -\infty$ , but  $F_{20} + F_{22} \rightarrow \log(16)/\pi$ , and recall that the conformal blocks are degenerate, eq. (150).

The probability reads:

$$P_{c=-2,\text{dense}}(\zeta) = \frac{K(1-\zeta)}{K(1-\zeta) + K(\zeta)} \quad (162)$$

$$= \frac{\pi}{\pi - \log\left(\frac{1-\zeta}{16}\right)} + \frac{\pi(1-\zeta)}{2\left(\pi - \log\left(\frac{1-\zeta}{16}\right)\right)^2} + O((1-\zeta)^2) . \quad (163)$$

When instead  $h \rightarrow 5/8$  (dilute case) we have  $F_{20} \rightarrow b/h^2 = 32/15$  and  $F_{22} \rightarrow -\infty$ . In this case the divergence of  $\mathcal{G}^0$ , eq. (151), compensates that of the OPE structure constant, and the result is finite:

$$P_{c=0,\text{dilute}}(\zeta) = \frac{S_2(1-\zeta)}{S_2(1-\zeta) + S_2(\zeta)} \quad (164)$$

$$= \frac{15\pi}{32}(1-\zeta)^2 + \frac{15\pi}{32}(1-\zeta)^3 \quad (165)$$

$$+ \frac{75\pi\left(12\log\left(\frac{1-\zeta}{16}\right) + 12\pi - 1\right)}{4096}(1-\zeta)^4 + O((1-\zeta)^5) . \quad (166)$$

We are not aware of a previous derivation of the above probability formulas. Note that since  $P(1-\zeta) = 1 - P(\zeta)$ , the same series plus the constant term holds for a very long rectangle ( $\zeta \rightarrow 0$ ) replacing  $1-\zeta$  by  $\zeta$ . We have already seen how rectangular amplitudes contain the OPE structure constants, and now we see that for logarithmic CFTs the indecomposability parameters (contained in the  $F$ -matrices) show up in geometric observables.

Note also that expressing the anharmonic ratio in terms of the modular parameter  $q$  through eq. (44)

$$\log(1-\zeta) = \log(16) + \log(\sqrt{q}) - 8\sqrt{q} + \dots \quad (167)$$

integer powers of  $\tau$  enter explicitly the expression of the probability. This feature is a consequence of the Jordan form of the transfer matrix in these cases.

More generally one could replace the ill-behaved conformal blocks in the logarithmic cases by a combination of them which has probabilistic interpretation and which is expected to be well defined even if the conformal blocks themselves are singular or degenerate. Unfortunately writing down explicitly such a probabilistic basis in the space of conformal blocks does not seem to be simple for higher number of line insertions. Indeed we do not know how to associate precisely a conformal block to a given propagation of lines (see discussion at the beginning of section 5.3), but more importantly, we do not know how to fix the normalization.

### 5.5 OPE coefficients and lattice crossing symmetry

Given a CFT rectangle boundary state  $|B_{ac}^b\rangle = \sum_s C_{ijs}^{abc} \sqrt{C_{ss0}^{aca}} |i^s{}_j\rangle$ , and the discretization of basis states introduced above in eq. (141), we can define the more general lattice boundary state as combination of lattice basis states

$$|B_{ac}^b\rangle_L = \sum_s D_{ijs}^{abc} |i^s{}_j\rangle_L. \quad (168)$$

We expect then that  $|B_{ac}^b\rangle_L \xrightarrow{(\text{FP})} |B_{ac}^b\rangle$  if

$$D_{ijs}^{abc} := C_{ijs}^{abc} \sqrt{C_{ss0}^{aca}} \frac{1}{\alpha_{ij}^s}. \quad (169)$$

We now question the universal character of  $\alpha$ . As the crossing symmetry of correlation functions (or rectangular amplitudes) is a powerful tool for constraining OPE structure constants in the continuum theory, we will see that also lattice crossing symmetry allows to derive constraints for the coefficients  $D$ 's appearing in eq. (168) and to infer about the universality of the coefficients  $\alpha$ 's.

Let us see concretely how to implement lattice crossing symmetry for the simplest non-trivial case of  $i = j = 1$ , corresponding to boundary fields inserting one line in each corner. For this situation all the possible CFT rectangle boundary states one has to consider are:

$$|B_{i,i+2}^{i+1}\rangle = C_{1,1,2}^{i,i+1,i+2} \sqrt{C_{220}^{i,i+2,i}} |1^2{}_1\rangle, \quad (170)$$

$$|B_{i,i}^{i\pm 1}\rangle = C_{1,1,0}^{i,i\pm 1,i} \sqrt{C_{000}^{iii}} |1^0{}_1\rangle + C_{1,1,2}^{i,i\pm 1,i} \sqrt{C_{220}^{iii}} |1^2{}_1\rangle, \quad (171)$$

where boundary labels  $\in \mathbb{N}$ . The discretization of the above basis boundary states follows from the discussion at the beginning of section 5.2 :

$$\frac{1}{\beta^{L/4}} \text{---}\overbrace{\cup \cdots \cup}^{\text{---}} \xrightarrow{(\text{FP})} \alpha_{11}^0 |1^0{}_1\rangle, \quad (172)$$

$$\frac{1}{\beta^{L/4-1/2}} \text{---}\overline{\cup \cdots \cup} \text{---} \xrightarrow{(\text{FP})} \alpha_{11}^2 |1^2{}_1\rangle. \quad (173)$$

Accordingly we introduce the discretizations

$$|B_{i,i+2}^{i+1}\rangle_L = \frac{D_{112}^{i,i+1,i+2}}{\beta^{L/4-1/2}} \text{---}\overline{\cup \cdots \cup} \text{---}, \quad (174)$$

$$|B_{i,i}^{i\pm 1}\rangle_L = \frac{D_{110}^{i,i\pm 1,i}}{\beta^{L/4}} \text{---}\overbrace{\cup \cdots \cup}^{\text{---}} + \frac{D_{112}^{i,i\pm 1,i}}{\beta^{L/4-1/2}} \text{---}\overline{\cup \cdots \cup} \text{---}. \quad (175)$$

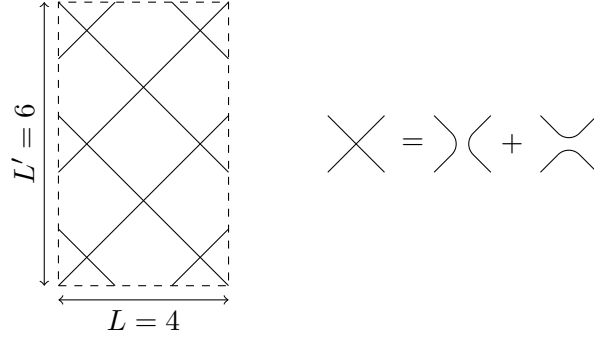


Figure 10: A lattice of size  $(L = 4) \times (L' = 6)$ . At each node we have the transfer matrix depicted on the right, equal to identity plus TL generators.

Now consider an  $L \times L'$  lattice as in figure 10, where each vertex corresponds to a node transfer matrix equal to the identity plus the Temperley Lieb generator.

A partition function on this lattice is specified by giving an initial and a final state, and computing the loop scalar product of the final state with the sum over all possible choices of node operators acting on the initial state. The universal part of the partition function in the continuum limit is a partition function in boundary CFT. The conformal boundary conditions are imposed by the choice of boundary states according to the identification of their continuum limit as discussed in section 5.2. Clearly one can decide to consider time flowing from bottom to top or from left to right; the equality of these two descriptions for each configuration is a constraint that we call lattice crossing symmetry and which allows for the determination of (ratios of) the coefficients  $D$ 's. See figure 11 for a picture of the resulting equation.

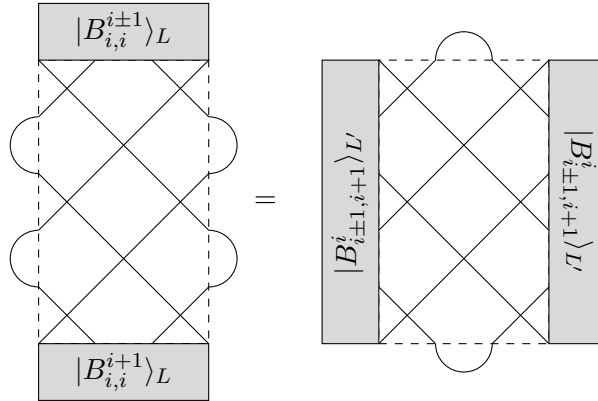


Figure 11: Equation imposing lattice crossing symmetry.

Consider first the case of boundary conditions  $i, i+1, i, i-1$  around the rectangle. Taking the identity operator acting in the bottom-top direction (or TL generators in the left-right direction) at every vertex, gives the equation

$${}_L\langle B_{i,i}^{i-1}|B_{i,i}^{i+1}\rangle_L = \beta^{L/2-1} {}_{L'}\langle B_{i+1,i-1}^i|\prod_{i=0}^{L'/2-1} e_{2i+1}|B_{i+1,i-1}^i\rangle_{L'} = 0, \quad (176)$$

leading to the first relation:

$$D_{110}^{i,i+1,i} D_{110}^{i,i-1,i} = -D_{112}^{i,i+1,i} D_{112}^{i,i-1,i}. \quad (177)$$

Then consider the case with  $i, i+1, i, i+1$  around the rectangle. Again taking identity in the bottom-top direction at every vertex gives

$${}_L\langle B_{i,i}^{i+1}|B_{i,i}^{i+1}\rangle_L = \beta^{L/2-1} {}_{L'}\langle B_{i+1,i+1}^i|\prod_{i=0}^{L'/2-1} e_{2i+1}|B_{i+1,i+1}^i\rangle_{L'}, \quad (178)$$

yielding:

$$\left(D_{110}^{i,i+1,i}\right)^2 + \left(D_{112}^{i,i+1,i}\right)^2 = \beta^{L/2-L'/2} \beta \left(D_{110}^{i+1,i,i+1}\right)^2. \quad (179)$$

Now, taking instead contractions in the bottom-top direction (identity for left-right direction) at every vertex gives

$$\beta^{L'/2-1} {}_L\langle B_{i,i}^{i+1}|\prod_{i=0}^{L/2-1} e_{2i+1}|B_{i,i}^{i+1}\rangle_L = {}_{L'}\langle B_{i+1,i+1}^i|B_{i+1,i+1}^i\rangle_{L'}, \quad (180)$$

yielding:

$$\left(D_{110}^{i+1,i,i+1}\right)^2 + \left(D_{112}^{i+1,i,i+1}\right)^2 = \beta^{L'/2-L/2} \beta \left(D_{110}^{i,i+1,i}\right)^2. \quad (181)$$

Defining

$$\mathcal{C}_{\pm}^i = \frac{D_{112}^{i,i\pm 1,i}}{D_{110}^{i,i\pm 1,i}}, \quad (182)$$

these equations imply:

$$\mathcal{C}_+^i = \sqrt{\frac{\beta^2}{1 + (\mathcal{C}_-^{i+1})^2} - 1}, \quad \mathcal{C}_+^i = -\frac{1}{\mathcal{C}_-^i}. \quad (183)$$

These are recursion relations for the coefficients  $\mathcal{C}$  with initial condition  $\mathcal{C}_+^0 = 0$ , and are independent of the system sizes  $L, L'$ . The solution of the recursion can be expressed in terms of Chebyshev polynomials of the second kind  $U_n(x)$  as:

$$\mathcal{C}_{\pm}^i = \pm \sqrt{\frac{U_{i\mp 1}\left(\frac{\beta}{2}\right)}{U_{i\pm 1}\left(\frac{\beta}{2}\right)}}. \quad (184)$$

The first few coefficients read explicitly

$$\mathcal{C}_-^1 = \sqrt{\beta^2 - 1}; \quad \mathcal{C}_+^1 = -\frac{1}{\sqrt{\beta^2 - 1}}, \quad (185)$$

$$\mathcal{C}_-^2 = \sqrt{\beta^2 - 2}; \quad \mathcal{C}_+^2 = -\frac{1}{\sqrt{\beta^2 - 2}}, \quad (186)$$

$$\mathcal{C}_-^3 = \sqrt{\frac{\beta^4 - 3\beta^2 + 1}{\beta^2 - 1}}; \quad \mathcal{C}_+^3 = -\sqrt{\frac{\beta^2 - 1}{\beta^4 - 3\beta^2 + 1}}, \dots \quad (187)$$

We now claim that these expressions are not restricted to the two cases solved above and indeed solve every possible constraint one can write down from switching the left-right and bottom-top descriptions of lattice partition functions. Using (169) and setting  $i = 1$ , we have that the ratio  $\alpha_{11}^2/\alpha_{11}^0$  is:

$$\frac{\alpha_{11}^2}{\alpha_{11}^0} = \frac{1}{\sqrt{\beta^2 - 1}} \frac{C_{112}^{101} \sqrt{C_{220}^{111}}}{C_{110}^{101} \sqrt{C_{000}^{111}}}. \quad (188)$$

Note that crossing symmetry only allows to determine  $\alpha$ 's up to a common constant.

As already remarked, if we had started with lattice boundary states differing from those we have used by local modifications (e.g. by allowing a finite number of arches between the through lines, etc.), we would expect that the continuum limit would be the same, but with different  $\alpha$ 's. For example, we could consider instead of eq. (172):

$$\frac{1}{\beta^{L/4}} \text{---} \cup \cup \dots \cup \text{---} \xrightarrow{(\text{FP})} \hat{\alpha}_{11}^0 | 1^0 1 \rangle. \quad (189)$$

If we start with different boundary states, the equations resulting from lattice crossing symmetry would be modified in general (e.g. if we use the boundary state above, eq. (179) will have an extra factor of  $\beta^2$  in the r. h. s. , similarly eq. (181)). The ratio of coefficients for boundary states with local modifications  $\hat{\alpha}_{11}^2/\hat{\alpha}_{11}^0$  should always be independent of system size and related to  $\beta$  and OPE constants, but in general different from (188). Since we expect more generally that  $\alpha_{ij}^s$  changes under a local modification of the microscopic state (e.g. by extra factors of  $\beta$  in the example above), it cannot be predicted by the CFT. Note that the “physical” states  $|B_{ac}^b\rangle_L$  defined in eq. (168) are normalized in order to obtain in the continuum the CFT states  $|B_{ac}^b\rangle$ , and the CFT partition functions (30), when taking overlaps.

The expression (188) can be simplified further using eq. (66) for  $i = j = k = l = 1$ ,  $a = c = 0$ ,  $b = d = 1$ ,  $r = 2$ :

$$(C_{110}^{101})^2 C_{000}^{111} F_{02} \begin{bmatrix} 1 & 1 \\ 1 & 1 \end{bmatrix} + (C_{112}^{101})^2 C_{220}^{111} F_{22} \begin{bmatrix} 1 & 1 \\ 1 & 1 \end{bmatrix} = 0, \quad (190)$$



and the explicit results (96) yield

$$\frac{\alpha_{11}^2}{\alpha_{11}^0} = \sqrt{\frac{\beta \Gamma\left(-\frac{8h_1}{3} - \frac{1}{3}\right) \Gamma\left(\frac{2}{3} - \frac{8h_1}{3}\right)}{(\beta^2 - 1) \Gamma\left(\frac{1}{3} - \frac{4h_1}{3}\right) \Gamma(-4h_1)}}. \quad (191)$$

In table 3 we check these results against numerical values obtained for  $p = 3, 4, 5$ , with  $p$  parametrizing the fugacity of loops as  $\beta = 2 \cos(\pi/(p+1))$ . Large sizes which we did not study would be needed to get more precise results, but nonetheless we find good agreement in these cases.

$p$	num	theo
3	0.70715(9)	$\simeq 0.70711$
4	0.68506(32)	$\simeq 0.69267$
5	0.66671(66)	$\simeq 0.68736$

Table 3: Comparison of the ratio  $\alpha_{11}^2/\alpha_{11}^0$  determined numerical (num) by fitting values for  $L = 10 \rightarrow 24$  and theoretically (theo) using eq. (191) for different values of  $p$ , parametrizing the weight of loops  $\beta = 2 \cos(\pi/(p+1))$ .

Now that we have determined the ratio  $\alpha_{11}^2/\alpha_{11}^0$  we can invert the reasoning and determine the OPE coefficients in terms of it from eq. (184):

$$\frac{C_{112}^{i,i\pm 1,i} \sqrt{C_{220}^{iii}}}{C_{110}^{i,i\pm 1,i} \sqrt{C_{000}^{iii}}} = \pm \sqrt{\frac{\beta \Gamma\left(-\frac{8h_1}{3} - \frac{1}{3}\right) \Gamma\left(\frac{2}{3} - \frac{8h_1}{3}\right)}{(\beta^2 - 1) \Gamma\left(\frac{1}{3} - \frac{4h_1}{3}\right) \Gamma(-4h_1)}} \sqrt{\frac{U_{i\mp 1}\left(\frac{\beta}{2}\right)}{U_{i\pm 1}\left(\frac{\beta}{2}\right)}}. \quad (192)$$

In particular the rectangle partition functions for  $\phi_1$  insertion in each corner can be explicitly written as (the functions  $\mathcal{G}$ 's are defined in section 3.2.2)

$$\begin{array}{c} i+1 \\ \bullet \\ i \end{array} \begin{array}{c} \square \\ \bullet \\ i+1 \end{array} \begin{array}{c} i+2 \\ \bullet \\ i \end{array} = A_i L^{c/4-8h_1} \eta^{-c/2} \theta_3^{16h_1} \mathcal{F}^2(1-z) \quad (193)$$

$$\begin{array}{c} i+1 \\ \bullet \\ i \end{array} \begin{array}{c} \square \\ \bullet \\ i+1 \end{array} \begin{array}{c} i \\ \bullet \\ i \end{array} = B_i L^{c/4-8h_1} \eta^{-c/2} \theta_3^{16h_1} \left( \mathcal{F}^0(1-z) + F_{02} \frac{\beta}{\beta^2-1} \frac{U_{i-1}\left(\frac{\beta}{2}\right)}{U_{i+1}\left(\frac{\beta}{2}\right)} \mathcal{F}^2(1-z) \right). \quad (194)$$

The constant of proportionality  $A_i, B_i$  can be read off from the general formula (31) and are given in terms of boundary OPE coefficients. We note that for the CFT describing loop models we are considering here, these coefficients are known and can be obtained by analytic continuation of the  $F$ -matrices for minimal models  $\mathcal{M}(p, p+1)$  [19].

## 6 Conclusion

In this work we have constructed CFT boundary states encoding rectangular geometries with different boundary conditions, and elucidated their relation with correlators of boundary conditions changing operators, completing the investigation initiated in [3]. We have developed in particular the geometrical interpretation in terms of lattice loop models, and we have derived new formulas for probabilities of self-avoiding walks. Remarkably, these formulas contain the indecomposability parameters of logarithmic CFTs in the expansion of the amplitudes.

In conclusion, the formalism developed in [3] and the present paper gives access to large classes of loop models partition functions on the rectangle. A further generalization should allow one, for instance, to obtain closed formulas for the average conductance of rectangles at the higher plateau transitions in the spin quantum Hall effect, along the lines of [4, 5].

**Acknowledgments:** We thank J. Dubail for useful discussions and earlier collaboration on a related work. This work was supported in part by a grant from the ANR Projet 2010 Blanc SIMI 4: DIME.

## A Useful formulas

We collect in this appendix definitions and useful properties of special functions appearing in the main part of the manuscript.

The theta functions we use are defined as:

$$\eta(\tau) = q^{1/24} \prod_{n=1}^{\infty} (1 - q^n) = \left( \frac{\theta_2(\tau)\theta_3(\tau)\theta_4(\tau)}{2} \right)^{1/3} \quad (195)$$

$$\theta_2(\tau) = \sum_{n \in \mathbb{Z}} q^{(n+1/2)^2/2} = 2 \frac{\eta(2\tau)^2}{\eta(\tau)} \quad (196)$$

$$\theta_3(\tau) = \sum_{n \in \mathbb{Z}} q^{n^2/2} = \frac{\eta(\tau)^5}{\eta(\tau/2)^2 \eta(2\tau)^2} \quad (197)$$

$$\theta_4(\tau) = \sum_{n \in \mathbb{Z}} (-1)^n q^{n^2/2} = \frac{\eta(\tau/2)^2}{\eta(\tau)}, \quad (198)$$

with  $q = e^{2\pi i \tau}$ ,  $\tau = L'/L$ . Denote by  $K$  the complete elliptic integral of the first kind with modulus  $k$  and  $K' := K(1 - k^2)$  its complementary, then  $\tau = iK'/(2K)$ . One has

$$k = \left( \frac{\theta_2(2\tau)}{\theta_3(2\tau)} \right)^2 = \frac{\theta_3(\tau)^2 - \theta_4(\tau)^2}{\theta_3(\tau)^2 + \theta_4(\tau)^2} = \left( \frac{\pi \theta_2(\tau)^2}{4K} \right)^2; \quad K = \frac{\pi}{4} (\theta_3(\tau)^2 + \theta_4(\tau)^2). \quad (199)$$

Modular properties of these theta functions are:

$$\eta(-1/\tau) = \sqrt{-i\tau}\eta(\tau) \quad (200)$$

$$\theta_2(-1/\tau) = \sqrt{-i\tau}\theta_4(\tau) \quad (201)$$

$$\theta_3(-1/\tau) = \sqrt{-i\tau}\theta_3(\tau) \quad (202)$$

$$\theta_4(-1/\tau) = \sqrt{-i\tau}\theta_2(\tau), \quad (203)$$

$$\eta(\tau+1) = e^{i\pi/12}\eta(\tau) \quad (204)$$

$$\theta_2(\tau+1) = e^{i\pi/4}\theta_2(\tau) \quad (205)$$

$$\theta_3(\tau+1) = \theta_4(\tau) \quad (206)$$

$$\theta_4(\tau+1) = \theta_3(\tau). \quad (207)$$

## B Boundary states for two one-leg insertions

We give here explicit expressions of basis boundary state  $|_1^0\rangle$  and  $|_1^2\rangle$  for generic  $c = 1 - 6/(p(p+1))$  up to level 8:

$$\begin{aligned} 4^{2h_1} |_1^0\rangle &= |0\rangle + \left(7 - \frac{24}{p+3}\right) L_{-2}|0\rangle \\ &+ \left(-\frac{40}{3p+5} + \frac{24}{p+3} - \frac{1}{2}\right) L_{-4}|0\rangle + \left(\frac{200}{9p+15} - \frac{48}{p+3} + \frac{19}{6}\right) L_{-2}^2|0\rangle \\ &- \frac{128(p+1)p^2}{3(p+3)(3p+5)(5p+7)} L_{-3}^2|0\rangle + \frac{(p(p(709p+769)-1665)+315)}{6(p+3)(3p+5)(5p+7)} L_{-4}L_{-2}|0\rangle \\ &+ \frac{(p(667-p(103p+331))-105)}{6(p+3)(3p+5)(5p+7)} L_{-2}^3|0\rangle + \frac{64(2p-1)p}{3(3p+5)(5p+7)} L_{-6}|0\rangle \\ &+ \frac{(p-9)(p(p(709p+481)-1761)+315)}{12(p+3)(3p+5)(5p+7)(7p+9)} L_{-8}|0\rangle + \frac{64p(p(6p^2+p-16)+9)}{(p+3)(3p+5)(5p+7)(7p+9)} L_{-6}L_{-2}|0\rangle \\ &+ \left(-\frac{80}{3p+5} - \frac{196}{5p+7} + \frac{324}{7p+9} + \frac{24}{p+3} + \frac{1}{8}\right) L_{-4}L_{-2}^2|0\rangle \\ &+ \left(\frac{800}{9(3p+5)} - \frac{1372}{3(5p+7)} + \frac{2916}{7(7p+9)} + \frac{4}{p+3} - \frac{11}{504}\right) L_{-2}^4|0\rangle \\ &- \frac{256p^2(p+1)}{3(3p+5)(5p+7)(7p+9)} L_{-5}L_{-3}|0\rangle \\ &+ \left(\frac{520}{9(3p+5)} + \frac{14896}{15(5p+7)} - \frac{8424}{7(7p+9)} - \frac{60}{p+3} + \frac{53}{1260}\right) L_{-4}L_{-2}^2|0\rangle \\ &- \frac{128(p-9)p^2(p+1)}{3(p+3)(3p+5)(5p+7)(7p+9)} L_{-3}^2L_{-2}|0\rangle + \dots, \end{aligned} \quad (208)$$

$$\begin{aligned}
4^{2h_1-h_2}|1^2\rangle &= |\phi_2\rangle + \frac{5p-1}{3p+1}L_{-2}|\phi_2\rangle - \frac{2(p+1)}{3p+1}L_{-1}^2|\phi_2\rangle \\
&+ \frac{34p^3+21p^2+44p-3}{60p^3+86p^2+40p+6}L_{-4}|\phi_2\rangle - \frac{16(p-2)p(p+1)}{(2p+1)(3p+1)(5p+3)}L_{-3}L_{-1}|\phi_2\rangle \\
&- \frac{p^2+34p-3}{30p^2+28p+6}L_{-2}^2|\phi_2\rangle + \frac{20p^3+58p^2+44p+6}{30p^3+43p^2+20p+3}L_{-2}L_{-1}^2|\phi_2\rangle - \frac{2(p+1)^2(2p+3)}{30p^3+43p^2+20p+3}L_{-1}^4|\phi_2\rangle \\
&+ \frac{64p(p(p(43p+96)+44)-21)+18}{9(2p+1)(3p+1)(3p+2)(5p+3)(7p+5)}L_{-6}|\phi_2\rangle \\
&+ \frac{16p(p+1)(p(p(17p-9)-48)+252)}{9(2p+1)(3p+1)(3p+2)(5p+3)(7p+5)}L_{-5}, L_{-1}|\phi_2\rangle \\
&+ \frac{p(p(p(8662p+12621)+1175)-11631)-5337+270}{18(2p+1)(3p+1)(3p+2)(5p+3)(7p+5)}L_{-4}L_{-2}|\phi_2\rangle \\
&- \frac{128p^2(p(5p+19)+6)}{9(3p+1)(3p+2)(5p+3)(7p+5)}L_{-3}^2|\phi_2\rangle \\
&+ \frac{p(p(65-p(970p+2159))+2997)+1833+90}{3(2p+1)(3p+1)(3p+2)(5p+3)(7p+5)}L_{-4}L_{-1}^2|\phi_2\rangle \\
&- \frac{16p(p+1)(p(p(123p-203)+144)+180)}{9(2p+1)(3p+1)(3p+2)(5p+3)(7p+5)}L_{-3}L_{-2}L_{-1}|\phi_2\rangle + \frac{p(269-p(97p+29))-15}{6(3p+1)(5p+3)(7p+5)}L_{-2}^3|\phi_2\rangle \\
&+ \frac{32p(p+1)^2(p(35p+52)+60)}{9(2p+1)(3p+1)(3p+2)(5p+3)(7p+5)}L_{-3}L_{-1}^3|\phi_2\rangle \\
&+ \frac{(p+1)(p(p(518p-151)-921)-90)}{9(2p+1)(3p+1)(3p+2)(7p+5)}L_{-2}^2L_{-1}^2|\phi_2\rangle \\
&- \frac{2(p+1)^2(p(7p(58p+1)-723)-270)}{9(2p+1)(3p+1)(3p+2)(5p+3)(7p+5)}L_{-2}L_{-1}^4|\phi_2\rangle \\
&+ \frac{4(p+1)^3(p(10p-17)-30)}{9(2p+1)(3p+1)(3p+2)(5p+3)(7p+5)}L_{-1}^6|\phi_2\rangle + \dots
\end{aligned} \tag{209}$$

## References

- [1] E. Ardonne and G. Sierra, *Chiral correlators of the Ising conformal field theory*, Journal of Physics A: Mathematical and Theoretical **43** (2010), no. 50, 505402.
- [2] M. Bauer and D. Bernard, *2D growth processes: SLE and Loewner chains*, Physics Reports **432** (2006), no. 34, 115–221.
- [3] R. Bondesan, J. Dubail, J. L. Jacobsen, and H. Saleur, *Conformal boundary state for the rectangular geometry*, Nuclear Physics B **862** (2012), no. 2, 553–575.
- [4] R. Bondesan, I. A. Gruzberg, J. L. Jacobsen, H. Obuse, and H. Saleur, *Exact Exponents for the Spin Quantum Hall Transition in the Presence of Multiple Edge Channels*, Phys. Rev. Lett. **108** (2012), 126801.
- [5] R. Bondesan, J. L. Jacobsen, and H. Saleur, *Edge states and conformal boundary conditions in super spin chains and super sigma models*, Nuclear Physics B **849** (2011), no. 2, 461–502.
- [6] P. Calabrese and J. Cardy, *Quantum quenches in extended systems*, Journal of Statistical Mechanics: Theory and Experiment **2007** (2007), no. 06, P06008.
- [7] J. Cardy, *Operator content of two-dimensional conformally invariant theories*, Nuclear Physics B **270** (1986), 186–204.
- [8] ———, *Boundary conditions, fusion rules and the Verlinde formula*, Nuclear Physics B **324** (1989), no. 3, 581–596.
- [9] ———, *Critical percolation in finite geometries*, Journal of Physics A: Mathematical and General **25** (1992), no. 4, L201.
- [10] ———, *Linking Numbers for Self-Avoiding Loops and Percolation: Application to the Spin Quantum Hall Transition*, Phys. Rev. Lett. **84** (2000), 3507–3510.
- [11] ———, *Conformal Invariance and Percolation* (March 2001), available at [arXiv:math-ph/0103018](https://arxiv.org/abs/math-ph/0103018).

- [12] J. Cardy and I. Peschel, *Finite-size dependence of the free energy in two-dimensional critical systems*, Nuclear Physics B **300** (1988), 377–392.
- [13] N. Diamantis and P. Kleban, *New percolation crossing formulas and second-order modular forms*, ArXiv e-prints (May 2009), available at <http://arxiv.org/abs/0905.1727>.
- [14] J. Dubail, J. L. Jacobsen, and H. Saleur, *Conformal field theory at central charge  $c = 0$ : A measure of the indecomposability ( $b$ ) parameters*, Nuclear Physics B **834** (2010), no. 3, 399–422.
- [15] J. Dubail and J.-M. Stéphan, *Universal behavior of a bipartite fidelity at quantum criticality*, Journal of Statistical Mechanics: Theory and Experiment **2011** (2011), no. 03, L03002.
- [16] B. Duplantier and F. David, *Exact partition functions and correlation functions of multiple Hamiltonian walks on the Manhattan lattice*, Journal of Statistical Physics **51** (1988), 327–434. 10.1007/BF01028464.
- [17] G. Felder, J. Fröhlich, J. Fuchs, and C. Schweigert, *Conformal Boundary Conditions and Three-Dimensional Topological Field Theory*, Phys. Rev. Lett. **84** (2000Feb), 1659–1662.
- [18] P. Di Francesco, P. Mathieu, and D. Sénéchal, *Conformal field theory*, Graduate texts in contemporary physics, Springer, 1997.
- [19] P. Furlan, A. C. Ganchev, and V.B. Petkova, *Fusion matrices and  $c < 1$  (quasi) local conformal theories*, International Journal of Modern Physics A (IJMPA) **05** (1990), no. 14, 2721–2735.
- [20] M. R. Gaberdiel, *An Algebraic approach to logarithmic conformal field theory*, Int. J. Mod. Phys. **A18** (2003), 4593–4638.
- [21] V. Gurarie and A. W. W. Ludwig, *Conformal Field Theory at central charge  $c=0$  and Two-Dimensional Critical Systems with Quenched Disorder*, ArXiv High Energy Physics - Theory e-prints (September 2004), available at [arXiv:hep-th/0409105](http://arxiv.org/abs/hep-th/0409105).
- [22] Y. Imamura, H. Isono, and Y. Matsuo, *Boundary States in the Open String Channel and CFT near a Corner*, Progress of Theoretical Physics **115** (2006), no. 5, 979–1002.
- [23] ———, *Boundary State of Superstring in Open String Channel*, Progress of Theoretical Physics **119** (2008), no. 4, 643–662.
- [24] N. Ishibashi, *The Boundary and Crosscap States in Conformal Field Theories*, Mod. Phys. Lett. **A4** (1989), 251.
- [25] E. V. Ivashkevich, *Correlation functions of dense polymers and  $c = -2$  conformal field theory*, Journal of Physics A: Mathematical and General **32** (1999), no. 9, 1691.
- [26] P. Kleban and I. Vassileva, *Domain boundary energies in finite regions at 2-D criticality via conformal field theory*, J. Phys. **A25** (1992), 5779–5787.
- [27] P. Kleban and D. Zagier, *Crossing Probabilities and Modular Forms*, Journal of Statistical Physics **113** (2003), 431–454.
- [28] David C. Lewellen, *Sewing constraints for conformal field theories on surfaces with boundaries*, Nuclear Physics B **372** (1992), no. 3, 654–682.
- [29] E. Lieb, T. Schultz, and D. Mattis, *Two soluble models of an antiferromagnetic chain*, Annals of Physics **16** (1961), no. 3, 407–466.
- [30] P. P. Martin, *Potts Models and Related Problems in Statistical Mechanics*, Series on Advances in Statistical Mechanics, World Scientific, 1991.
- [31] G. Moore and N. Seiberg, *Lectures on RCFT*, Physics, geometry, and topology, 1990, pp. 263–361.
- [32] P. A. Pearce, J. Rasmussen, and J.-B. Zuber, *Logarithmic minimal models*, Journal of Statistical Mechanics: Theory and Experiment **2006** (2006), no. 11, P11017.
- [33] N. Read and H. Saleur, *Associative-algebraic approach to logarithmic conformal field theories*, Nuclear Physics B **777** (2007), no. 3, 316–351.
- [34] I. Runkel, *Boundary structure constants for the A-series Virasoro minimal models*, Nuclear Physics B **549** (1999), no. 3, 563–578.

- [35] A. D. Sokal, *The multivariate Tutte polynomial (alias Potts model) for graphs and matroids* (March 2005), 54 pp., available at [0503607](#).
- [36] X. Wu, N. Izmailian, and W. Guo, *Finite size behaviors of critical Ising model on a rectangle with free boundaries*, ArXiv e-prints (2012), available at [1207.4540](#).
- [37] Z. Yin, *Conformal Invariance on Orbifolds and Excitations of Singularity*, Modern Physics Letters A **24** (2009), 2089–2097.